



A new version of the CNRM Chemistry-Climate Model, CNRM-CCM: description and improvements from the CCMVal-2 simulations

M. Michou¹, D. Saint-Martin¹, H. Teyssèdre¹, A. Alias¹, F. Karcher¹, D. Olivié^{1,*}, A. Voldoire¹, B. Josse¹, V.-H. Peuch¹, H. Clark², J. N. Lee³, and F. Chéroux¹

¹GAME/CNRM, Météo-France, CNRS – Centre National de Recherches Météorologiques, Toulouse, France

²Laboratoire d’Aérologie, Université de Toulouse, CNRS, Toulouse, France

³Jet Propulsion Laboratory, California Institute of Technology, Pasadena, USA

* now at: Dept. of Geosciences, University of Oslo, Norway

Received: 18 May 2011 – Published in Geosci. Model Dev. Discuss.: 31 May 2011

Revised: 22 September 2011 – Accepted: 23 September 2011 – Published: 6 October 2011

Abstract. This paper presents a new version of the Météo-France CNRM Chemistry-Climate Model, so-called CNRM-CCM. It includes some fundamental changes from the previous version (CNRM-ACM) which was extensively evaluated in the context of the CCMVal-2 validation activity. The most notable changes concern the radiative code of the GCM, and the inclusion of the detailed stratospheric chemistry of our Chemistry-Transport model MOCAGE on-line within the GCM. A 47-yr transient simulation (1960–2006) is the basis of our analysis. CNRM-CCM generates satisfactory dynamical and chemical fields in the stratosphere. Several shortcomings of CNRM-ACM simulations for CCMVal-2 that resulted from an erroneous representation of the impact of volcanic aerosols as well as from transport deficiencies have been eliminated.

Remaining problems concern the upper stratosphere (5 to 1 hPa) where temperatures are too high, and where there are biases in the NO₂, N₂O₅ and O₃ mixing ratios. In contrast, temperatures at the tropical tropopause are too cold. These issues are addressed through the implementation of a more accurate radiation scheme at short wavelengths. Despite these problems we show that this new CNRM CCM is a useful tool to study chemistry-climate applications.

1 Introduction

Three-dimensional atmospheric circulation models with a fully interactive representation of stratospheric ozone chemistry are known as stratosphere-resolving Chemistry-Climate Models (CCMs). They are key tools for the attribution and projection of stratospheric ozone changes arising from the combined effects of changes in the amounts of greenhouse gases (GHG) and ozone-depleting substances (ODS). These sophisticated models are a compromise between representing multiple dynamical, physical and chemical processes and the setting up of long-term simulations which are computationally expensive. They have been and continue to be extensively evaluated (Eyring et al., 2006; SPARC, 2010 and references therein). The latest published assessment of the ozone depletion (WMO/UNEP, 2010) is primarily based on their conclusions and states that there is now new and stronger evidence of the effect of stratospheric ozone changes on Earth’s surface climate, and of the effects of climate change on stratospheric ozone.

We present in this study results of a modelling activity that lead to the definition and implementation of a new version of the Météo-France Centre National de Recherches Météorologiques (CNRM) CCM, “CNRM-CCM”. This modelling activity has built upon the WCRP/SPARC (World Climate Research Project/Stratospheric Processes and their Role in Climate) CCMVal-2 (Chemistry-Climate Model Validation) activities, analyses and outcomes. CNRM contributed to CCMVal-2 with a first version of its CCM, so-called CNRM-ACM (ARPEGE Coupled with MOCAGE),



Correspondence to: M. Michou
(martine.michou@meteo.fr)

along with seventeen other modelling groups. CCMVal-2 evaluated a comprehensive number of processes to assess the capability of CCMs to reproduce past observations in the stratosphere. Furthermore, these CCMs were utilised to predict the future evolution of stratospheric ozone and climate under one particular scenario (SPARC, 2010). The evaluated processes cover radiation, stratospheric dynamics, transport in the stratosphere, stratospheric chemistry, upper troposphere and lower stratosphere (UTLS), natural variability of stratospheric ozone, long-term projections of stratospheric ozone, and the effects of the stratosphere on the troposphere. On the basis of this comprehensive review, a number of deficiencies in the various CCMs have been identified. In this paper we present the developments that have been implemented at the CNRM institute and results are analysed here.

The remainder of this paper is structured as follows: in Sect. 2, we describe the new version of the model, given its heritage and its own specifications. In Sect. 3, we present the simulations performed and the results obtained, outlining the progress made from the main shortcomings identified in the first version of the CNRM CCM. A synthesis discussion concludes the paper.

2 The CNRM-CCM Model heritage, description and runs

2.1 CNRM-CCM heritage

The new model version CNRM-CCM is an evolution of CNRM-ACM both in terms of their underlying General Circulation Model (GCM), as well as in the way these CCMs deal with the chemistry part through the interactions between chemical, radiative and dynamical processes. CNRM-ACM had been developed as a combination of the GCM ARPEGE-Climat (version 4.6) and a stratospheric version of the MOCAGE atmospheric Chemistry-Transport Model (CTM).

2.1.1 GCM component

The global atmospheric model, ARPEGE-Climat, originates from the ARPEGE/IFS (Integrated Forecast System) numerical weather prediction model developed jointly by Météo-France and the European Center for Medium-range Weather Forecast (ECMWF). Version 3, very close to version 4.6, has been used in various climate sensitivity experiments (see for instance Douville et al., 2002 and Volodire and Royer, 2005), and results from simulations with version 4.6 appear in Swingedouw et al. (2010) and Johns et al. (2011). A detailed description of the model can be found in Déqué (2007).

CNRM-ACM uses a “high top” version of ARPEGE-Climat, with 60 levels in a hybrid sigma-pressure coordinate system spanning the atmosphere from the surface to 0.07 hPa (24 levels above 100 hPa). ARPEGE-Climat uses a semi-lagrangian scheme with a two time-level discretization. The physical schemes include turbulent vertical diffusion and dry

convection as described in Ricard and Royer (1993), and deep convection as described in Bougeault (1985). Radiation follows Morcrette (1991) with 9 bands in the long-wave (LW) and 2 in the short-wave (SW) part of the spectrum. Six types of aerosols are considered by the radiation scheme and monthly climatologies of optical depth are ingested (Tegen et al., 1997), with evolving yearly climatologies for volcanic (Ammann et al., 2007) and sulphate sources. The model includes a subgrid-scale orographic scheme based on Lott and Miller (1997) and Lott (1999). It also contains a non-orographic gravity-wave drag parametrization (GWD, Bossuet et al., 1998), which links the GWD to the tropospheric convection. The model also includes the land model ISBA first developed by Noilhan and Planton (1989) (see Mahfouf et al., 1995), upgraded by the snow cover formulation of Douville et al. (1995), and the boundary layer scheme of Louis et al. (1982), modified by Mascart et al. (1995).

2.1.2 CTM component

The stratospheric chemistry parametrization is the stratospheric version of the MOCAGE model that is the multi-scale 3-D CTM of Météo-France which represents processes from the regional to the planetary scale, and extends from the surface up to the middle stratosphere. An evaluation of the present-day chemical climatology of MOCAGE appears in Teyssèdre et al. (2007).

The chemistry model (see Lefèvre et al., 1994) calculates the evolution of 55 species using 160 gas-phase reactions. Reaction rate coefficients are taken from the recommendations of Sander et al. (2006). To solve chemical equations, the model uses the popular “family” method, (see Brasseur et al., 1998; Morgenstern et al., 2010a), and considers the O_x , HO_x , NO_x , ClO_x and BrO_x families.

The photolysis rates are calculated at every time step using a look-up table from the Tropospheric and Ultraviolet Visible (TUV) model (Madronich and Flocke, 1998) tabulated for 81 altitudes, 7 total ozone columns and 27 solar zenith angles; furthermore photolysis rates are modified according to cloudiness following Brasseur et al. (1998). Solar cycle effects are included updating photolysis tables each month from the phase of the 11-yr cycle.

The chemistry is computed down to the 560 hPa model level while for higher pressures the mixing ratios of a number of species (namely N_2O , CH_4 , CO , CO_2 , $CFC11$, $CFC12$, $CFC113$, CCl_4 , CH_3CCl_3 , CH_3Cl , $HCFC22$, CH_3Br , $H1211$, $H1301$, O_x , O_3 , Cly , Bry , NO_y) are relaxed towards evolving global mean surface abundances (see SPARC (2010) for the ozone depleting substances and greenhouse gases, and the CNRM-CCM technical documentation for the other compounds). Explicit wash-out of chemical species is not considered in this stratospheric version of the model.

Three types of particles are considered in the heterogeneous reactions (Carslaw et al., 1995), liquid stratospheric aerosols and Polar Stratospheric Clouds (PSCs) that include

water ice and NAT (Nitric Acid Trihydrate). Monthly distributions of sulfate aerosols are externally imposed, with inter-annual variability mostly driven by large volcanic eruptions.

2.1.3 GCM-CTM interface

The GCM and CTM components of CNRM-ACM are coupled via the three-dimensional fields of wind, temperature, ozone and water vapor. The GCM provides the horizontal and vertical winds, temperature and tropospheric humidity for the CTM, which returns the 3-D ozone field back to the GCM in order to calculate radiation fluxes and heating rates. The chemically active constituents are transported by the semi-Lagrangian advection scheme maintained by MOCAGE (Williamson and Rasch, 1989). A simple correction scheme is applied in order to guarantee total mass conservation during transport (see details and evaluation in Josse et al., 2004).

In order to meet the time schedule of the CCMVal-2 activity, CNRM-ACM simulations were performed using two different horizontal resolutions: the one of the GCM was based on a T42 spectral truncation while that of the chemistry model was based on a T21 truncation (the corresponding Gaussian grid has 64 longitudes and 32 latitudes i.e. 5.6° spaced grid points). It has to be noted that such a T21 resolution is lower than the ones for which the CTM MOCAGE has been thoroughly validated (typically 2° and higher resolutions, as in Williams et al., 2010); issues regarding transport were thus not fully unexpected.

2.1.4 CNRM-ACM evaluation

CNRM-ACM has been evaluated in a number of publications: as stated at the introduction of this article, the SPARC CCMVal report (SPARC, 2010) is an overall effort to assess CCMs performance, both individually and collectively. In addition, CCMVal-2 articles published so far concern (1) a qualitative and quantitative evaluation of the overall stratospheric climate and variability of the CCMs (Butchart et al., 2010); (2) performances of the CCMs in the tropical and extra-tropical UTLS with regard to tropopause temperature and pressure, water vapour and ozone, and trends over the 21st century (Gettelman et al., 2010) and further analysis of the extra-tropical UTLS in Hegglin et al. (2010); (3) the evolution of ozone, including model simulations of the spring Antarctic ozone, over the past 40 yr and the 21st century. Projections of ODS and GHG as stated by the A1b IPCC scenario are analysed in Austin et al. (2010a), the decline and recovery of total column ozone over all regions of the globe in Austin et al. (2010b), while Oman et al. (2010) present a multi-model assessment of the factors driving the stratospheric ozone evolution over the 21st century; (4) Morgenstern et al. (2010b) address the question of how changes to ozone and long-lived greenhouse gases impact the Northern Annular Mode; (5) Son et al. (2010) examine how the

tropospheric circulation of the Southern Hemisphere (SH) is impacted by changes in stratospheric ozone, and in particular ozone depletion in late spring, and establish a quantitative relationship between these two quantities.

This comprehensive review of the CCMVal-2 model characteristics identified strengths and deficiencies, in particular in CNRM-ACM. We detail in Sect. 3 the main results provided for CNRM-ACM, focusing on its deficiencies, some of which were major. We show in parallel the corresponding outputs of the CNRM-CCM model. In the next Sect. (2.2), we describe the changes that led to the design of CNRM-CCM. These changes concern both the GCM part of the models as well as the way the GCM and the chemistry interact. In contrast, the stratospheric chemistry parametrization scheme (gas phase and heterogeneous reactions), although its code was fully rewritten to comply with the coding requirements of the GCM, can be considered as unchanged between CNRM-ACM and CNRM-CCM.

2.2 CNRM-CCM specifications

The CNRM-CCM GCM is the one used at CNRM for the Coupled Model Intercomparison Project Phase 5 simulations (CMIP5, see <http://cmip-pcmdi.llnl.gov/cmip5/experiment-design.html>) performed in preparation of the Intergovernmental Panel on Climate Change (IPPC) Assessment Report 5 (Volodire et al., 2011). A number of minor differences exist between the dynamical/physical components of the CNRM-ACM GCM (ARPEGE-Climat version 4.6) and that of the CNRM-CCM GCM (ARPEGE-Climat version 5.2) including adjustments of the horizontal diffusion, of the gravity wave drag parametrisation and of the time step of the model. However, a major evolution concerns their radiation scheme, both in the SW spectrum with 2 and 6 bands respectively, and above all in the LW spectrum. The LW component in ARPEGE version 5.2 is an adaptation of the Rapid Radiative Transfer Model (RRTM) scheme (Morcrette et al., 2001) that allows the representation of both the true cloud fraction and the spectrally defined emissivities and transmissivities in each of 16 different spectral bands. Seven gases are considered as absorbers, H_2O , CO_2 , O_3 , CH_4 , N_2O , CFC11, and CFC12 whose 3-D distributions are provided by the chemistry module of CNRM-CCM (see below). Accuracy in the calculation of fluxes and cooling rates consistent with the best line-by-line models is obtained (Morcrette et al., 2001).

Finally on the radiation scheme, the GCM part of the CNRM-ACM code included an incorrect calculation of heating rates because of volcanic aerosols which resulted in anomalous dynamical and chemical evolutions of the lower stratosphere for several years after major eruptions. This has been corrected in the CNRM-CCM code.

A second major difference between CNRM-ACM and CNRM-CCM is that the chemistry of CNRM-CCM is so-called “on-line”: the simulation of gaseous chemistry has been directly integrated within the GCM code. Chemical

routines are a subset of the entire set of model routines, and chemical species are considered as prognostic variables of the model. The advection scheme is thus the same for meteorological and for chemical variables, avoiding inconsistencies with transport. In this stratospheric configuration of the CNRM-CCM model, convective and turbulent transports of chemical species are not considered. One has to note that state-of-the art CCMs rarely consider tropospheric chemistry because of computer resources (among the 18 models of CCMVal-2 only 3 represented tropospheric chemical reactions, see Morgenstern et al., 2010a). The chemistry routines of CNRM-CCM are integrated within the physics part of the model and therefore the chemistry is activated at each time-step of the physics. Another aspect of chemistry fields being variables of the model is that chemical evolutions are resolved on the model grid. So in contrast with CNRM-ACM runs, CNRM-CCM runs were done on a T42 Gaussian grid both for dynamics and chemistry.

Additional details on ARPEGE-Climat appear in <http://www.cnrm-game.fr/spip.php?article124>, with technical and scientific documentation. A technical documentation on the CNRM-CCM chemical subroutines is also available.

2.3 Simulations analysed

As the objective of this paper was to build upon CCMVal-2, we performed CNRM-CCM simulations as defined in Eyring et al. (2008) and SPARC (2010). We analyse here results from a transient simulation identical to CCMVal-2 REF-B1 in terms of the period simulated (1960–2006), and the external forcings used (SSTs, ODSs, GHGs, aerosol forcing, solar irradiance). As in the CNRM-ACM REF-B1 simulation, the Quasi Biennial Oscillation (QBO) was not imposed on CNRM-CCM. A lot of research activity has been devoted to this major mode of variability of the equatorial stratosphere. Baldwin et al. (2001) review in a detailed and didactic way the knowledge acquired since its discovery in 1960, and their summary indicates that its effects range from modulating the stratospheric flow from pole to pole, to affecting the variability of the mesosphere up to 85 km and the strength of Atlantic hurricanes. Changes in atmospheric dynamics in turn affect the distribution of chemical compounds, including O_3 , H_2O , and CH_4 . The QBO also has an effect on the breakdown of the wintertime stratospheric polar vortices and the severity of high-latitude ozone depletion. Indirectly, through impacting polar vortices it then has an effect on the surface meteorology. Dynamical processes also influence temperatures which in turn impact on the chemistry of ozone because of the temperature dependence of the reaction rates. The natural variability of O_3 has been analysed in a specific chapter of the SPARC (2010) report. For instance, amplitude of the global ($60^\circ S$ – $60^\circ N$) column ozone variations in link with the QBO has been estimated to amount to ~ 4 DU, to be compared with an annual cycle where the natural variability has an amplitude of ~ 12 DU. However, analysis of the

CCMVal-2 model results suggest a range of sensitivity of the ozone to the QBO. The simulation of the QBO still remains a challenge for CCMs as it requires a high enough vertical resolution, an accurate parametrisation of the gravity waves that has been adjusted specifically to the model to interact in a realistic way with its synoptic-scale waves, and a realistic stratospheric Brewer-Dobson circulation in particular its tropical upwelling.

Although we chose to present one CNRM-CCM simulation only, we performed during the course of the CNRM-CCM development four additional REF-B1 type simulations that differed slightly from the one presented in this paper, either in the formulation of the chemistry or in the version of the GCM. All the diagnostics shown below lead to the same conclusions for all five simulations, except otherwise depicted (see Sect. 3.2.5). We also include in our analysis the outputs of the CCMVal-2 REF-B1 models as an indication of the state-of-the-art CCM modelling.

3 Results

The CCMVal-2 community agreed upon a very large number of diagnostics that illustrate its in-depth effort to assess the performances of CCMs. The results shown in this paper represent a small selection of these diagnostics. They concern mainly the stratosphere as neither CNRM-ACM nor CNRM-CCM consider the specific processes of the mesospheric (e.g. ion chemistry) or the tropospheric chemistry (because of its significant computer added cost), and they report on the ability of the CNRM models to reproduce the climatology of the recent past including a few aspects of the depiction of the past ozone depletion. We focus on the major shortcomings of the CNRM-ACM model, and present also a panel of satisfactory results for both models.

3.1 Validation data sets

A summary of the diagnostics analysed in this study together with their accompanying reference data sets appears in Table 1. Further details on these reference data sets is provided below.

3.1.1 Meteorological reanalyses

The first validation data set we considered is the extensively used ERA-40 reanalysis (Uppala et al., 2005) which covers the period September 1957–August 2002. We also used the ERA-Interim product (1989–present, Simmons et al., 2006) that combines a number of modifications made since the realisation of ERA-40 reported in Uppala et al. (2008) and Dee and Uppala (2009). Progress has been largely due to improvements in modelling and data assimilation achieved at ECMWF since the production of ERA-40 and includes for the stratosphere, a more realistic Brewer Dobson circulation,

Table 1. Diagnostics considered in this study.

Process	Diagnostics	Variables	Observations
Dynamics	High lat. strat. biases Winter, spring	T (Temperature)	ERA-40; Uppala et al. (2005) ERA-Interim; Simmons et al. (2006) NCEP, UKMO reana.; Eyring et al. (2006)
	Easterlies at 60° S SH and NH Night Polar Jet	U (zonal wind) U	ERA-40, ERA-Interim ERA-40
Transport	Tape recorder	H_2O	HALOE; Grooß and Russel (2005)
	Latitu. profiles at 0.5, 10 and 50 hPa	Age of air	Various; Eyring et al. (2006)
	Vert. and latitu. profiles	CH_4	HALOE
	Seasonal cycles at 100, 200 hPa and at 40° N–60° N, 60° S–40° S	O_3 , H_2O HNO_3	HALOE, MIPAS; SPARC (2010) MIPAS
UTLS	Seasonal cycles at 100 hPa Equator	T	ERA-40, ERA-Interim
		O_3 , H_2O	HALOE
	Latitu. profiles ANN, DJF, JJA	Tropo. pressure	ERA-40, ERA-Interim
Natural variability	Anom. at 50 hPa	T	ERA-40, ERA-Interim
Chemistry	Vert. and latitu. profiles	H_2O , O_3 , HCl	HALOE
	Time ser. at 50 hPa, 80° S	Cl	Various; Eyring et al. (2006)
	Seasonal cycles at 50, 1hPa and at 30° N–60° N, 30° S–60° S, 15° S–15° N	CH_4 , H_2O , O_3 , HCl HNO_3 , NO_2 , N_2O_5 BrO	HALOE MIPAS SCIAMACHY; SPARC (2010)
		$ClONO_2$	MIPAS
		CO	MLS; Lee et al. (2011)
	Total column 1980–1990, 1990–2000	O_3	BSv2.7; Bodeker et al. (2005)

as well as a better cycle of specific humidity in the tropical lower stratosphere. In addition, zonal-mean stratospheric temperatures show some marked differences between ERA-Interim and ERA-40, particularly at the higher levels where only radiance data are available for assimilation. We derived for both reanalyses, monthly temperature and zonal winds on the T42 horizontal grid of our simulations (about 2.8°) over 22 levels up to 1 hPa. We excluded the highest levels as the reanalyses are not constrained by observations in the mesosphere (Bechtold et al., 2009).

3.1.2 HALOE/UARS satellite observations

The Grooß and Russel (2005) climatology, that is the reference for a number of diagnostics, has been built from the data of the HALOE instrument onboard the Upper Atmosphere Research Satellite (UARS) that observed mixing ratios of important trace species in the stratosphere for more than ten years, starting in 1991. A zonal climatology has been compiled using the results of the version 19 retrieval software over a 5° latitude grid and 22 pressure levels from 316 to 0.1 hPa. We considered here mixing ratios of O_3 , H_2O , CH_4 , and HCl . Seasonal dependence is taken into account with

monthly data derived from November 1991–August 2002 observations. The most recent data since September 2002 have not been included in this climatology, since in 2002 a very unusual major warming occurred in Antarctica, and as observations have been less frequent after 2002. HALOE has been validated against a variety of measurements; generally, the accuracy of the retrievals decreases near the tropopause (Grooß and Russel, 2005 and references therein).

3.1.3 NIWA total column ozone

The assimilated National Institute of Water and Atmospheric Research (NIWA) data set combines satellite-based ozone measurements from four Total Ozone Mapping Spectrometer (TOMS) instruments, three different retrievals from the Global Ozone Monitoring Experiment (GOME) instruments, and data from four Solar Backscatter Ultra-Violet (SBUV) instruments. Comparisons with the global ground-based World Ozone and Ultraviolet Data Center (WOUDC) Dobson spectrophotometer network have been used to remove offsets and drifts between the different data sets to produce a global homogeneous total ozone column data set that combines the advantages of good spatial coverage of satellite

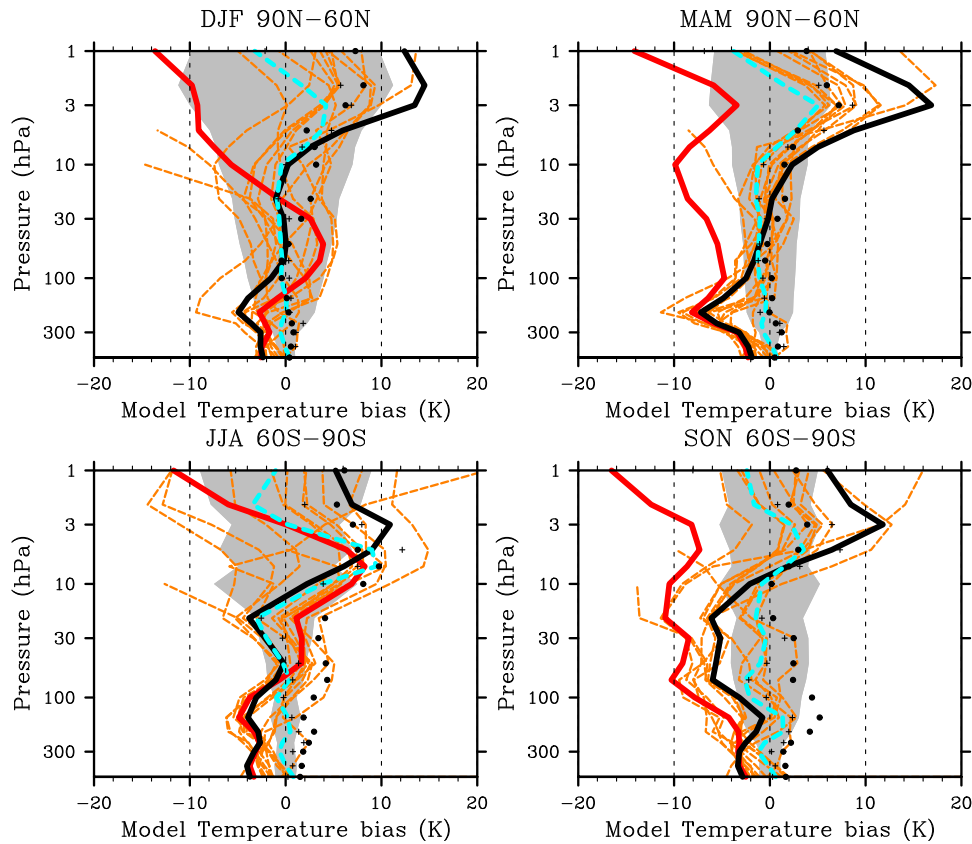


Fig. 1. Temperature biases over two latitude ranges, 90° N– 60° N (first row) and 60° S– 90° S (second row), and two seasons, winter (left column) and spring (right column). Biases are relative to the ERA-40 1980–2001 monthly reanalysis, for CNRM-ACM (red line), CNRM-CCM (black line) and CCMVal-2 REF-B1 models (dashed orange lines), and for ERA-Interim (dashed cyan line), NCEP (dots), and UKMO (crosses) reanalyses. The grey area shows ERA-40 ± 1 standard deviation.

data with good long-term stability of ground-based measurements. We used in this study version 2.7 of the so-called “patched” monthly data, available from <http://www.bodekerscientific.com/data/total-column-ozone>. Data cover the years 1979 to present at 1.25° (longitude) by 1° (latitude) resolution. For further details on the NIWA data set see Bodeker et al. (2005).

3.1.4 Other satellite observations

Observations shown in a couple of diagnostics include some of the satellite monthly climatologies that appear in Chapter 6 of SPARC (2010). They allow a first rough validation of a number of chemical species of the model, and are a personal communication from S. Dhomse, 2011. These climatologies have been derived from MIPAS/ENVISAT measurements for HNO_3 , N_2O_5 , NO_2 , and ClONO_2 , from SMR/ODIN measurements for HNO_3 , and from SCIAMACHY/ENVISAT measurements for BrO . We used zonal fields on the 31 vertical levels (1000 to 0.1 hPa) of the CCMVal-2 simulation exercise (SPARC, 2010). A zonal climatology of CO from MLS/AURA is also presented as a

reference data set (Lee et al., 2011). It has been built from six years of observations (2005–2010) (retrieval software version 2.2) onto 35 pressure levels (316 up to 0.002 hPa) and 43 latitudes (4° bands). MLS CO compares satisfactorily with ACE-FTS/SCISAT-1 and SMR/ODIN, except for a known large bias (a factor of 2) in the upper troposphere.

3.2 Main shortcomings of CCRM-ACM and corresponding CCM-CCM results

The statements below (in italics), that synthesize the main shortcomings of the CNRM-ACM simulations for CCMVal-2, have been extracted from various chapters of SPARC (2010) i.e. “Stratospheric dynamics” (see Sects. 3.2.1 and 3.2.2), “Transport” (see Sects. 3.2.3 and 3.2.4), “UTLS” (see Sects. 3.2.5, 3.2.6 and 3.2.7) and “Natural variability of stratospheric ozone” (see Sect. 3.2.8).

3.2.1 Stratospheric dynamics: temperature

CNRM-ACM produces a stratospheric mean state with significant biases in temperature. Figure 1 shows climatological

temperature biases relative to the ERA-40 reanalysis over the high latitudes of the Northern and Southern hemispheres (NH and SH) both in winter and spring. As these polar temperatures are important to represent correctly the ozone depletion due to PSCs, biases presented are those from the longest period with large ozone depletion available in the simulations (1980–2001). This diagnostic has been analysed for CCMVal-1 simulations (Eyring et al., 2006) and for CCMVal-2 ones (SPARC, 2010). Figure 1 includes the biases of various monthly reanalysis climatologies, NCEP and UKMO (over 1980–1999 and 1992–2001 respectively, see references in Eyring et al., 2006), and ERA-Interim (1989–2001) in addition to the CCMVal-2 and CNRM-CCM biases.

As in Eyring et al. (2006), a first contrast between the upper and the lower stratosphere can be noted, with the range of temperature biases reported in reanalyses being much larger in the upper atmosphere. A second contrast is evident between the two hemispheres with the cold bias of a large number of CCMVal-2 models in spring being much more extensive for the SH. There are some improvements in CNRM-CCM over CNRM-ACM. For example, in the lower to mid stratosphere, most biases have been reduced and in particular the cold biases in spring in both hemispheres where CNRM-ACM was clearly an outlier. The reduction in bias amounts to 8 K in MAM at 20 hPa for instance. CNRM-CCM reproduces ERA-40 particularly well in the 100–30 hPa layer of the northern latitudes, and it fits ERA-Interim in the 50–5 hPa layer of JJA. Between 5 and 1 hPa, differences between CNRM-CCM and CNRM-ACM are striking, this layer being generally too cold in CNRM-ACM and too warm in CNRM-CCM. CNRM-CCM is more in line with the CCMVal-2 models and with the NCEP and UKMO reanalyses, the disagreement between reanalyses amounting up to 10 K.

The change in radiative scheme between CNRM-ACM and CNRM-CCM certainly contributes to this evolution of the stratospheric temperatures. Morcrette et al. (2001) reports on the impact of replacing the LW FMR15 scheme (ARPEGE-Climat version 4.6) with RRTM (ARPEGE-Climat version 5.2). In summary, RRTM has shown an essentially positive impact over a large range of parameters, in particular for the surface radiation and the temperature in the stratosphere. Impacts right below the tropopause for temperature and humidity, as well as on convection in the tropics have also been noticed (see Morcrette et al., 2001 for details on changes in a number of radiative fields).

Climatological biases in temperature calculated relative to the first 20 yr of REF-B1, i.e. 1960–1980 (shown in the Supplement as Fig. S4) are quite different from those calculated over 1980–2001 (shown in Fig. 1), except for DJF between 90° N–60° N. In the 5–1 hPa layer in MAM between 90° N–60° N, most models are within the \pm ERA-40 standard deviation, apart from CNRM-ACM (10 K too cold) and CNRM-CCM (10 K too warm). In the SH (both for JJA and SON), most models show now positive biases in the 100–10 hPa layer (between 2 and 10 K), but in this case CNRM-CCM

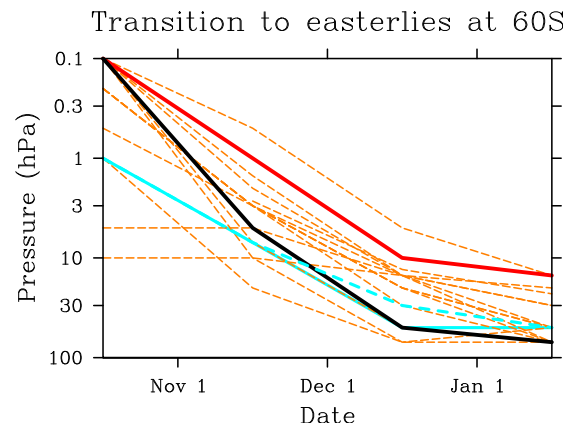


Fig. 2. Date of transition to easterlies at 60° S computed from the climatological (1980–2001) monthly zonal-mean zonal winds, for ERA-40 (cyan solid line), ERA-Interim (dashed cyan line), CNRM-ACM (red line), CNRM-CCM (black line) and CCMVal-2 REF-B1 models (dashed orange lines).

is among the closest to ERA-40. This outlines the interaction between ozone chemistry and temperatures, as well as the complexity of mechanisms over the various parts of the stratosphere that result in varying model performances.

Temperatures depicted in SON 60° S–90° S are closely linked to the transition from westerlies to easterlies at 60° S. We determined this transition by looking as in Eyring et al. (2006), at the mean seasonal cycle in the monthly zonal winds (1980–2001, see Fig. 2). The monthly mean is assumed valid for the 15th of every month, with linear interpolations in between the 15th of two consecutive months, but SPARC (2010) and references herein indicate that similar conclusions would be obtained from daily data. The ERA-40 and ERA-Interim reanalyses are plotted, and while the transition was delayed by around three weeks for CNRM-ACM, that of CNRM-CCM is much closer to reanalyses. This is consistent with a warmer spring stratosphere in the SH.

Finally for this analysis on stratospheric temperatures, we examined as in Fig. 3.1 of SPARC (2010), the stratospheric profiles of the mean annual biases (1980–1999) relative to ERA-40 over 90° S–90° N. Whilst CNRM-ACM was clearly an outlier for pressures lower than 200 hPa, with a persistent cold bias throughout the stratosphere, CNRM-CCM has no systematic bias throughout this atmospheric region, its absolute bias is lower than 4 K up to 5 hPa, and its largest bias is +10 K at 3 hPa (see Fig. S5 in the Supplement).

3.2.2 Stratospheric dynamics: wind

CNRM-ACM has significant biases in jet strength and position. It has particularly large biases in the NH, positioning its mean jet too far equator-ward. Stratospheric profiles of the strength and latitudinal position of the maximum of the zonal wind in DJF and JJA (1980–2001) are shown in Fig. 3,

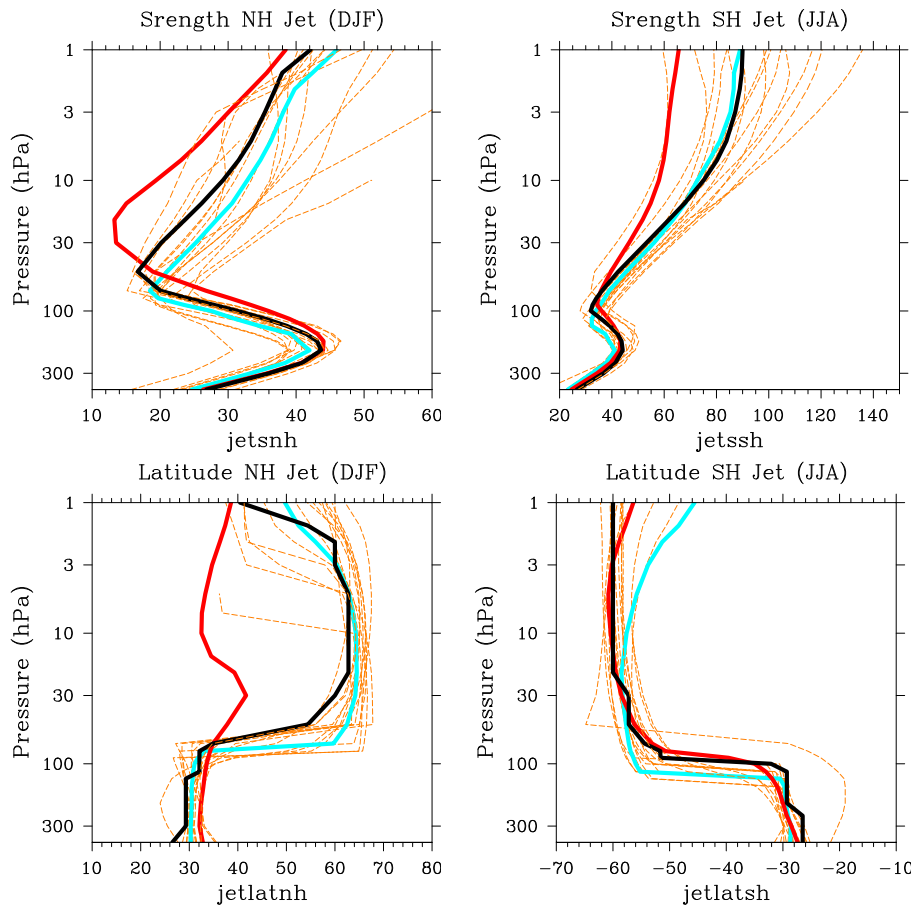


Fig. 3. Strengths (m s^{-1}) and latitudes of the maximum of the climatological zonal wind in DJF (first column) and JJA (second column). Climatologies (1980–2001) are for ERA-40 (cyan line), CNRM-ACM (red line), CNRM-CCM (black line), and CCMVal-2 REF-B1 models (dashed orange).

for ERA-40, CCMVal-2 models and CNRM-CCM. In the NH, SPARC (2010) indicate that CCMVal-2 models perform generally “extremely well” with the exception of a few models, one of which is CNRM-ACM. In CNRM-CCM however, both strength and position now appear to be correctly simulated. In the SH, CNRM-ACM weaknesses were less striking. CNRM-CCM performs similarly to CNRM-ACM with regards to the position of the jet and like most models fails to reproduce the observed tilt of the jet between 10 and 1 hPa. The strength of the jet in CNRM-CCM compares very well with ERA-40, in contrast with the other CCMVal-2 models which exhibit large biases of $\pm 20 \text{ m s}^{-1}$ or more in the upper stratosphere. Further evidence in the reduction of biases in the zonal wind, going from CNRM-ACM to CNRM-CCM, during the four seasons, appears in Fig. S10 of the Supplement.

3.2.3 Transport: tape recorder and age of air

The tape recorder and the age gradient of CNRM-ACM both indicate very rapid ascent in the Tropical Lower Stratosphere. ... The mean ages are very young everywhere, consistent with very fast net vertical transport. A number of diagnostics help to evaluate the transport characteristics of a model over regions where specific circulation processes occur (tropical ascent, tropical-extratropical mixing, integrated processes affecting mid-latitude composition, polar processes, see chapter 5 of SPARC, 2010). Transport determines to a large extent the distribution of long-lived species that in turn affect the entire chemistry of the stratosphere. We present in this paragraph three diagnostics extracted from those in Eyring et al. (2006) and SPARC (2010): information on the tropical ascent that should have limited horizontal mixing can be obtained from the vertical propagation of the annual cycle in water vapour (the so-called tape recorder), while the mean age of air at various pressures provides information on the overall transport throughout the stratosphere.

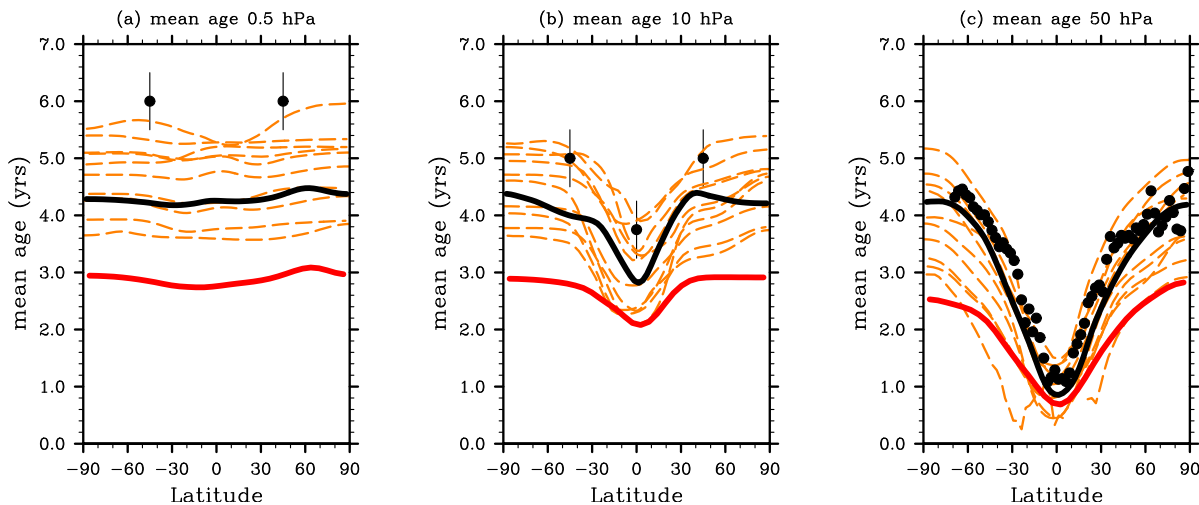


Fig. 4. Mean age of air at (a) 0.5, (b) 10, and (c) 50 hPa, observations (black dots $\pm 1\sigma$, set text), CNRM-ACM (red line), CNRM-CCM (black line) and CCMVal-2 REF-B1 models (dashed orange lines). Model outputs are from the 1980–2001 period.

Quality of the transport can also be confirmed by diagnostics on CH₄ as its chemistry is rather simple and should be correctly accounted for in models.

We analysed the deviation of the mean (1992–2001) water vapour mixing ratio from the monthly mean profile averaged over 10° S–10° N for the HALOE observations and model simulations (see Fig. S6 in the Supplement). Differences among models may result from multiple causes, including different advection schemes (see SPARC, 2010 and references therein for a description of these schemes), different tropopause temperatures, different ascent rates and mixing across the subtropical barriers. The CNRM-CCM tape recorder appears closer to observations than that of CNRM-ACM which exhibits an unusual pattern over this ten-year period in the alternation of wetter and drier conditions, certainly linked to errors in the sensitivity to volcanic eruptions (see below Sect. 3.2.7). The peak to peak amplitude of CNRM-CCM in the lower stratosphere appears reasonable but its ascent rate is too fast, with a lag of 3 months at about 30 hPa to be compared to 10 months for observations (phase lag as defined in Eyring et al., 2006, not shown).

The mean age of air is defined as the mean time that a stratospheric air mass has been out of contact with the well-mixed troposphere. Various methods can be used to compute the mean age of air, and in the CNRM simulations we considered an inert tracer whose concentration between 10° S–10° N and at 500 hPa increased linearly with time. Zonally averaged mean ages at 0.5, 10 and 50 hPa appear in Fig. 4, with observations from aircraft, balloon and satellite measurements as in Eyring et al. (2006), and model outputs. Although still too young by 1.5 yr at 0.5 hPa and by 0.6 yr at 10 hPa, CNRM-CCM is closer to observations than CNRM-ACM by about 1.5 yr at both levels. At 10 hPa, CNRM-CCM

is near the lower envelope of observations and comparable to the mean of the models. This is in agreement with the fact that the vertical propagation of tropical water vapour was too fast.

At 50 hPa, the improvement between CNRM-CCM and CNRM-ACM at mid and high latitudes is striking, and the mean age from CNRM-CCM fully superimposes observations, which is not the case for many models. Tropical (10° S–10° N) and mid-latitude (35° N–45° N) mean ages changed respectively from 1.7 (CNRM-ACM) to 2.4 yr (CNRM-CCM) and from 2.6 to 4.0 yr at 20 hPa (not shown). The mean age in CNRM-CCM is on the low end but within the 1 standard deviation of the mean of the observations (see Fig. 5.5 of SPARC, 2010).

CH₄ diagnostics also reflect largely the skill of transport representation in models. As in Fig. 5 of Eyring et al. (2006), we examined (see Fig. S7 in the Supplement) climatological zonal profiles, at selected latitudes, months, and pressure levels, for both model outputs and observations. The climatologies refer to the years 1992–2001 that correspond to the HALOE observations. Some spread between models appears, more evident in the polar regions at 50 hPa. CNRM-ACM values are generally closer to observations than those of most models. The largest differences between CNRM-ACM and CNRM-CCM appear at high latitudes, with for CNRM-CCM a degraded profile in the 30–10 hPa region at 77° N in March, and better ones in the same layer at 77° S in October as well as at northern high latitudes 50 hPa in March. Otherwise, CNRM-CCM and CNRM-ACM perform quite similarly, and overall these diagnostics do not reveal any weakness in the CNRM simulations.

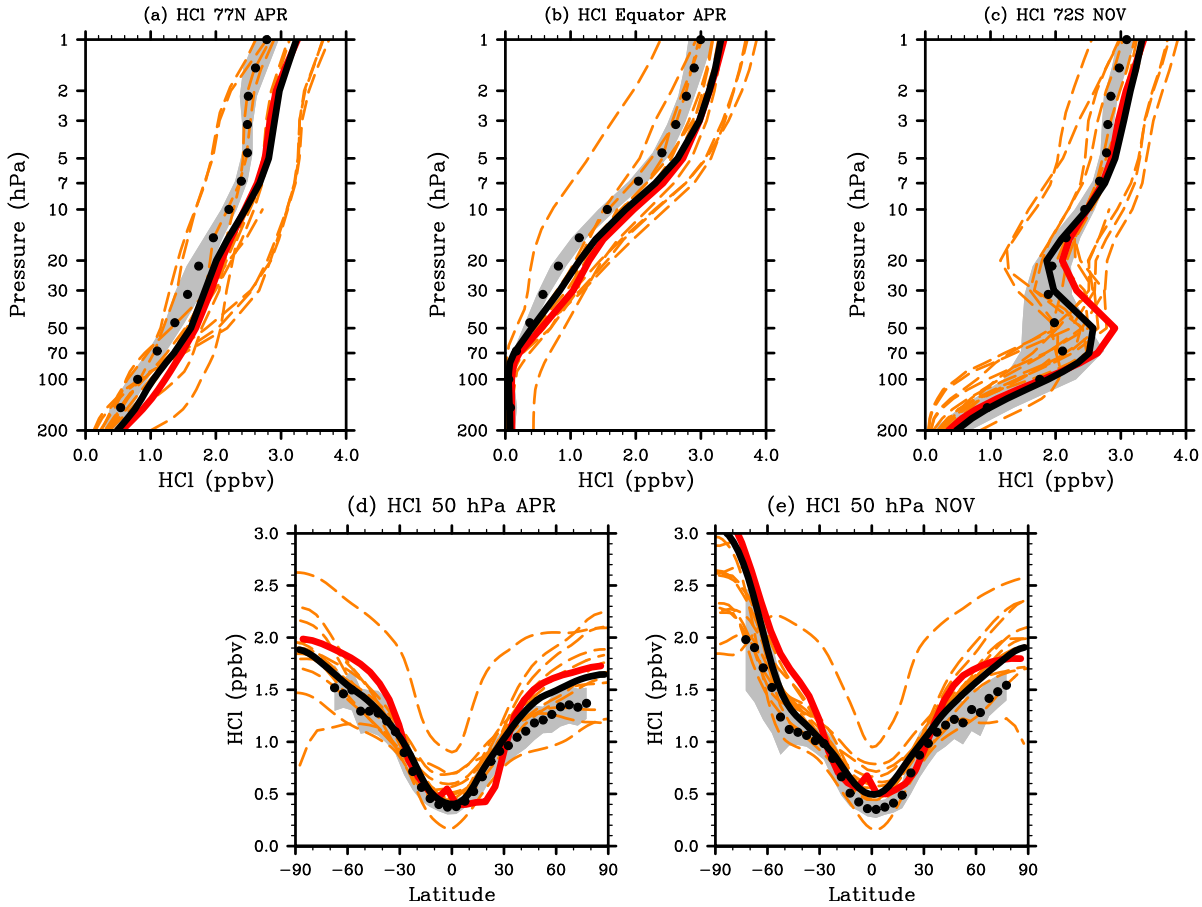


Fig. 5. Climatological (1992–2001) zonal-mean HCl mixing ratio (ppmv), for HALOE observations (black dots, with grey area showing $\pm 1\sigma$), CNRM-ACM (red line), CNRM-CCM (black line), and CCMVal-2 REF-B1 models (dashed orange lines). Vertical profiles at (a) 77° N in April, (b) 0° N in April, and (c) 72° S in November. Zonal-means at 50 hPa in (d) April and (e) November.

3.2.4 Transport: Cl_y

Overall, in spite of a very fast tracer-derived circulation, indications of significant vertical diffusion, and the absence of a high latitude transport barrier, compensating errors allow this model (CNRM-ACM) to produce realistic levels of Cl_y in the Antarctic Lower Stratosphere.

As the number of Cl_y observations is rather limited (Eyring et al., 2006), and since HCl is a major component of Cl_y in the upper stratosphere, we evaluate the chlorine content of the model using HCl profiles (see Fig. 5). For the high latitudes plots, we plotted the highest latitudes for which observations were available (this remark applies also to Figs. 7 and 11). CNRM-CCM mixing ratios are quite comparable to those from CNRM-ACM, and somewhat closer to HALOE observations in some cases, for instance in the Southern lower stratosphere (see panel c). Further evaluation of Cl_y is provided by the time series of mixing ratios in the lower southern polar stratosphere (50 hPa, October, see Fig. S8 in the Supplement). CNRM-CCM and CNRM-ACM

profiles are very similar and correspond to the high end of the model envelope that matches the two observations available, in 2000 and 2005 (see Eyring et al., 2006). These satisfactory results for CNRM-CCM should be underlined, given the spread of the CCMVal-2 outputs, given the changes in some transport characteristics between CNRM-ACM and CNRM-CCM, and given that chemistry remained unchanged between CNRM-ACM and CNRM-CCM. This seems to indicate that the chemistry is the main driver of the evolution of Cl_y in the Antarctic Lower Stratosphere.

3.2.5 Tropical UTLS

CNRM-ACM exhibits some significant problems with tropical transport. The tropopause is cold and high, with more water vapour than would be implied by the temperatures. Figure 6 compares mean annual cycles of temperature and water vapour from the model with those from ERA-40 (1980–2001 climatology) and from HALOE (1992–2001), respectively.

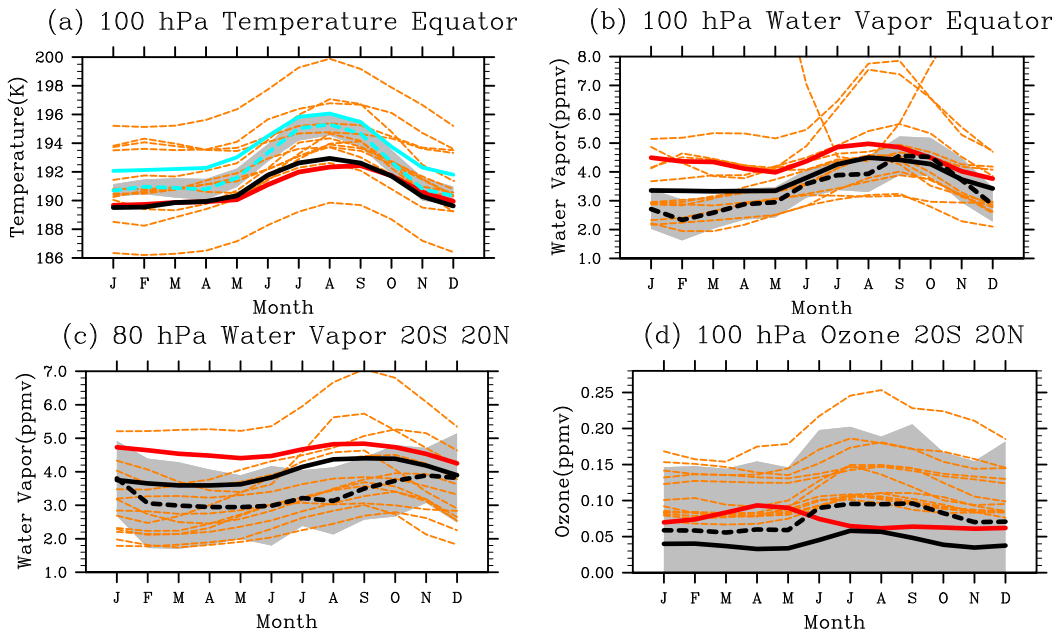


Fig. 6. Zonal tropical climatologies with “observations”, ERA-40 (cyan line), ERA-Interim (dashed cyan line, $\pm 1\sigma$ 1989–2001), and HALOE observations (dashed black line, $\pm 1\sigma$, 1992–2001): (a) temperature at Equator 100 hPa; (b) H_2O at Equator 100 hPa; (c) H_2O at $20^\circ S$ – $20^\circ N$ 80 hPa; and (d) O_3 at $20^\circ S$ – $20^\circ N$ 100 hPa. Models are also shown, CNRM-ACM (red line), CNRM-CCM (black line), and CCMVal-2 REF-B1 models (dashed orange lines). Note that in the second row, $\pm 3\sigma$ is shaded, as in SPARC (2010) Figs. 7.9 and 7.10.

These cycles are close to the Equatorial tropopause (100 hPa, see Eyring et al., 2006), or correspond to the entry point of the tape recorder (80 hPa, $20^\circ S$ – $20^\circ N$, see SPARC, 2010).

For temperatures, noting that a common systematic error concerns tropical lower stratospheric temperatures (SPARC, 2010), CNRM-CCM is more similar than CNRM-ACM to ERA-40 with a slightly more pronounced seasonal cycle that has a maximum in August. The permanent negative bias throughout the year is reduced from an upper limit (in July) of -3.8 K for CNRM-ACM to -3.2 K for CNRM-CCM. Figure 6 also shows temperatures for ERA-Interim (1989–2001 period) that are systematically lower than those of ERA-40, from 0.8 K in August to 1.5 K in November. ERA-Interim fits radiosonde observations better than ERA-40 at 100 hPa (see Randel et al., 2004), and if we now compare CNRM-CCM to ERA-Interim the negative bias is -2.4 K in July and August and -0.5 K in November. However, CNRM-CCM temperatures underestimate the mean minus 1σ of ERA-Interim except in October–November–December (see Fig. 6) and the amplitude of its annual cycle is not large enough. Interestingly, this seasonal cycle of the temperature is quite sensitive to the description of the chemistry and/or to small adjustments of the GCM. The five CNRM-CCM REF-B1 simulations performed (see Sect. 2.3) have seasonal cycles that differ, depending on the month by up to 1 K (see Fig. S3 in the Supplement).

Concerning water vapor, CNRM-CCM better fits observations than CNRM-ACM, with mixing ratios within the

uncertainties of the observations for the two diagnostics presented, which is not the case for CNRM-ACM, and a larger and thereby realistic annual cycle. The maximum of this annual cycle occurs a couple of months too early. Figure 7 gives further insight on the quality of the model water vapor field throughout the stratosphere. The five plots of this figure, vertical profiles at the polar latitudes in spring and at the Equator in March, or zonal-means at 50 hPa in March and October, illustrate the large spread in the models’ H_2O mixing ratios. Generally, CNRM-CCM is among the closest models to the observations in all the diagnostics shown. We can however note that the zonal mean in Fig. 7e is too flat, which is related to too much water vapor entering the stratosphere in March (see Fig. 7b). Anomalies in the CNRM-CCM phase of the tape recorder (see Sect. 3.2.3) may also prevent the model from reproducing the observations.

Differences in temperature and water vapor fields in the tropical lower stratosphere are closely linked to differences in the ozone field which is affected by both transport and chemistry and which is important in terms of radiative feedback. Cariolle and Morcrette (2006) provided quantitative estimates of the impact of changes in the O_3 field in the IFS simulations. These estimates are of special interest to us as the underlying GCM of CNRM-CCM is a climate version of the IFS model and as these estimates were done with a linearized version of the CNRM-CCM radiative code. Cariolle and Morcrette (2006) concluded that a reduction in O_3 in the range of 10–20 % in the lower stratosphere, that implies less

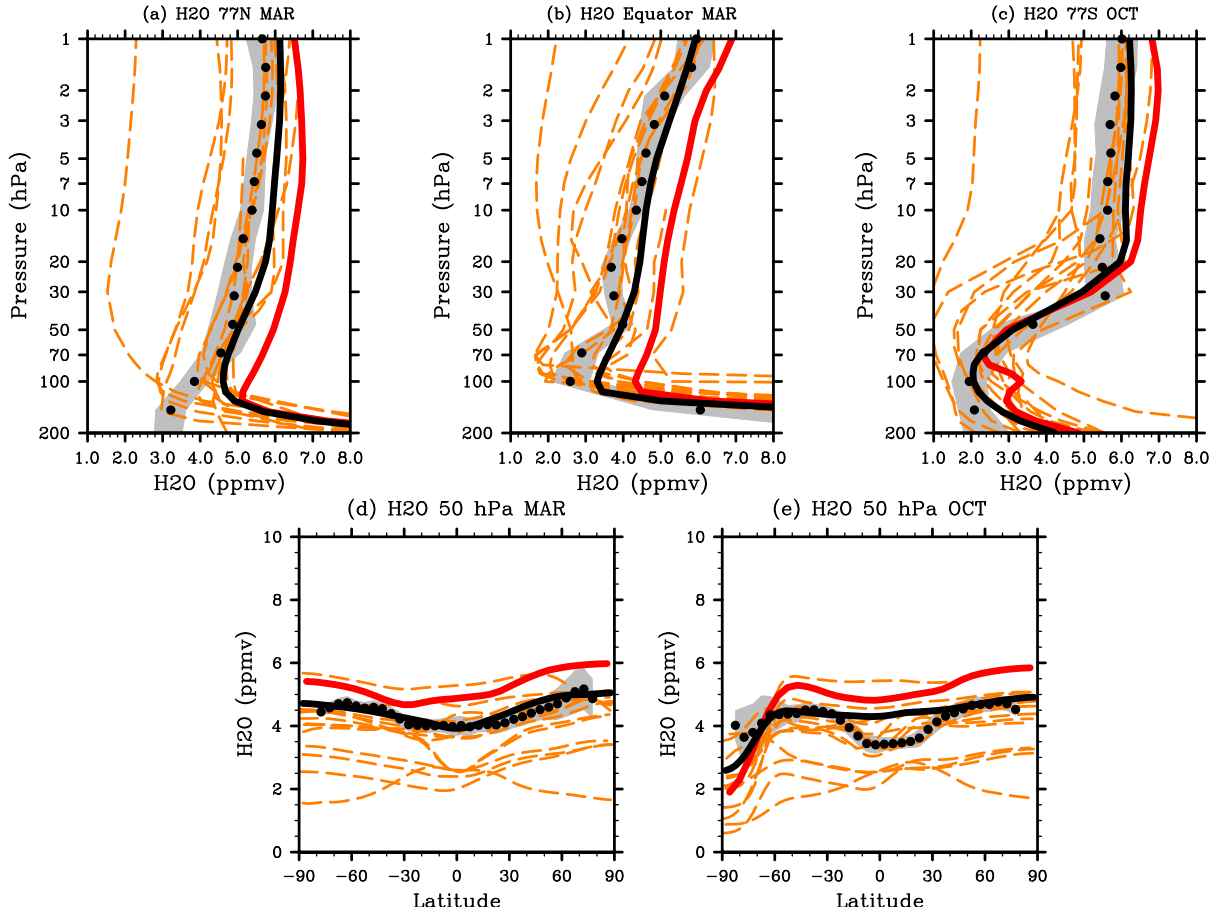


Fig. 7. Climatological (1992–2001) zonal-mean H_2O mixing ratio (ppmv), for HALOE observations (black dots, with grey area showing $\pm 1\sigma$), CNRM-ACM (red line), CNRM-CCM (black line), and CCMVal-2 REF-B1 models (dashed orange lines). Vertical profiles at (a) 77°N in March, (b) 0°N in March, and (c) 77°S in October. Zonal-means at 50 hPa in (d) March and (e) October.

UV absorption, along with an increase in the upper troposphere of 20 % which then filters part of the upward IR radiation and prevents its absorption by O_3 in the lower stratosphere, resulted in the lower stratosphere cooling by up to 3 K.

Figure 6d illustrates the dispersion of the mean annual cycles of O_3 at 100 hPa, 20°S – 20°N . Most models are within the 3σ of the HALOE mean (a range of variability that reflects the uncertainties at this level, see SPARC, 2010). CNRM-CCM O_3 mixing ratios are the lowest but the shape of its annual cycle is correct, which is an improvement over the CNRM-ACM outputs and is coherent with the improvements seen in Fig. 6a, b and c going from CNRM-ACM to CNRM-CCM.

3.2.6 Extra-tropical UTLS

Also in the extra-tropics, CNRM-ACM shows major deficiencies in both the dynamical and the transport and mixing diagnostics. Extra-tropical tropopause pressure is too low...

These deficiencies go along with too low HNO_3 in the SH, and too high H_2O in the NH at 200 hPa.

Figure 8 presents the climatological zonal tropopause pressure, for the two seasons DJF and JJA and the annual mean (1980–1999). The annual mean of CNRM-CCM is much closer to ERA-40 than that of CNRM-ACM, with differences lower than 40 hPa at all latitudes. The improvement between CNRM-ACM and CNRM-CCM is particularly visible at mid-latitudes where CCMVal-2 model biases are generally quite large, and is evident in the two seasons, with an exception however for the high latitudes of the winter hemisphere.

SPARC (2010) indicate that the seasonal cycles of O_3 , H_2O and HNO_3 give an indication of the quality of the underlying large-scale transport and mixing processes in the extra-tropical UTLS. Figure 9 shows the mean annual cycles of these species at two pressure levels (100 and 200 hPa), and two latitude bands (40°N – 60°N , 60°S – 40°S) with HALOE and MIPAS (Hegglin et al., 2010) observations for O_3 and H_2O , and MIPAS observations for HNO_3 .

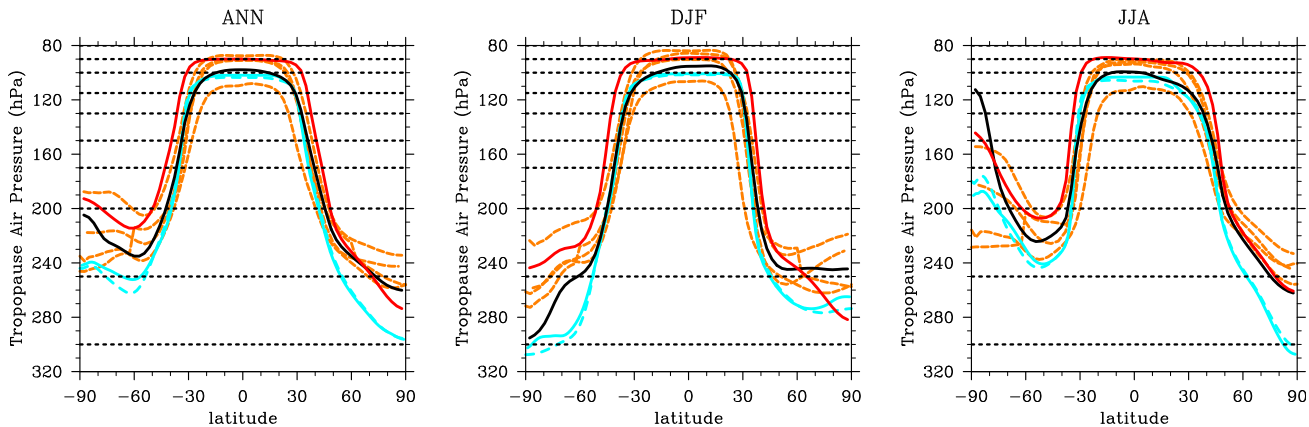


Fig. 8. Climatological zonal tropopause pressure (hPa), annual mean (left column), DJF (middle column) and JJA (right column). 1980–1999 values (except for ERA-Interim) for ERA-40 (cyan line), ERA-Interim (1989–2008, dashed cyan line), CNRM-ACM (red line), CNRM-CCM (black line) and CCMVal-2 REB-B1 models (dashed orange lines). Dotted horizontal lines represent the CCMVal-2 vertical model resolution around the tropopause.

For O_3 , the seasonal cycles of CNRM-CCM are in the range of those of the CCMVal-2 models and compare better with observations than the cycles of CNRM-ACM with larger yearly amplitude. In contrast, CNRM-ACM appears as an outlier in all four O_3 diagrams. As with most models at 100 hPa in the 60° S–40° S latitude band, CNRM-CCM overestimates O_3 observations compared with HALOE and MIPAS which both provide quite similar climatologies. Note that at 200 hPa the two observed O_3 climatologies shown differ by at least 0.05 ppmv and up to 0.18 ppmv.

CNRM-CCM H_2O is also closer to observations than CNRM-ACM H_2O and comparable to the mean of the models. At 200 hPa, the model mean largely overestimates observations as well as the amplitude of their annual cycle. However, these H_2O plots reveal that observations of H_2O in the UTLS region where gradients are large are still an issue, MIPAS mixing ratios being notably larger than HALOE mixing ratios, for instance by 7.5 ppmv at 200 hPa 40° S–60° S. Moreover, Hegglin et al. (2010) indicate that there is some evidence that the MIPAS H_2O at 200 hPa (let alone the HALOE H_2O at 200 hPa) might be too low, especially during summer. More measurements are required to evaluate model H_2O in the UTLS.

As for HNO_3 , we note that an error within the implementation of the heterogeneous chemistry in CNRM-ACM has been corrected in CNRM-CCM. Therefore, we will not comment on the CNRM-ACM HNO_3 any further. As for CNRM-CCM HNO_3 , while the annual cycles appear satisfactory in three out of the four cases presented in Fig. 9, the 200 hPa 60° S–40° S case is problematic: CNRM-CCM fails to simulate the annual cycle and even depicts an opposite cycle. Some sensitivity tests suggest that the problem is linked to the sedimentation process at latitudes higher than 60° S that seems too large, in link to too cold temperatures. Too low

HNO_3 transported to the 40° S–60° S latitudes prevents then the augmentation of HNO_3 mixing ratios as depicted by the observations.

3.2.7 Natural variability: temperature

The tropopause response to volcanic events is very large, and the secular trend is also larger than other models due to problems with volcanic aerosol heating.

The volcanic aerosol heating error in CNRM-ACM generated excessive lower stratospheric heating very rapidly after the volcanic eruption, followed for a couple of years by an excessive cooling (see Fig. 10 that represents anomalies of the annual global temperature at 50 hPa relative to the 1980–1989 period). This error led to problems with a number of CCMVal-2 dynamical diagnostics, and chemical as a consequence, for CNRM-ACM. It had a pronounced effect on temperatures in the tropical lower stratosphere and also on trends in cold point tropopause or trends in tropopause pressure over 1960–2000 (see chapter 7 of SPARC, 2010). Analysis of the natural variability of CNRM-ACM stratospheric ozone was also greatly impacted by this error.

The problem has been solved in CNRM-CCM and its temperature anomalies linked to volcanic eruptions follow those of ERA-40, they are larger than the anomalies of most models in the case of minor eruptions and smaller in the case of a large eruption such as the Pinatubo (1991) eruption (see Fig. 10). The temperature trend per decade calculated over the 1960–2001 period that was $-2.26 \text{ K decade}^{-1}$ for CNRM-ACM is -0.82 for CNRM-CCM. The latter corresponds to the trend of ERA-40 which in turn is close to the trend from radiosondes (see Austin et al., 2009). Over this 47-yr period, most CCMVal-2 models have a trend higher than $-0.7 \text{ K decade}^{-1}$ at 50 hPa (reduced cooling) which

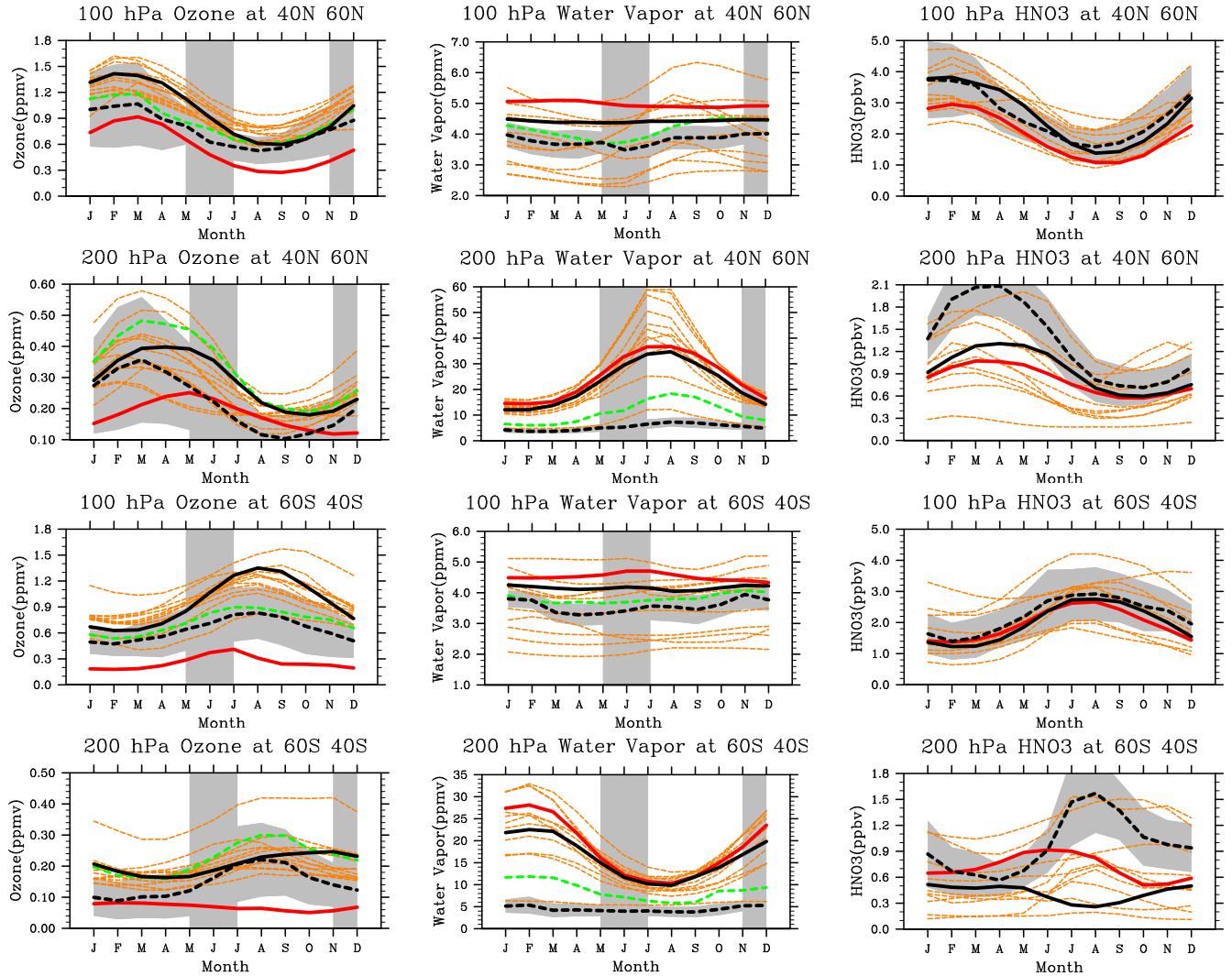


Fig. 9. Mean annual cycle for O₃ (ppmv, left column), H₂O (ppmv, middle column), and HNO₃ (ppbv, right column) for 40° N–60° N 100 hPa (first row), 40° N–60° N 200 hPa (second row), 60° S–40° S 100 hPa (third row), and 60° S–40° S 200 hPa (fourth row). Observations (dashed black line, $\pm 1\sigma$, grey bar where σ missing) HALOE for O₃ and H₂O, and MIPAS for HNO₃, CNRM-ACM (red line), CNRM-CCM (black line) and CCMVal-2 REF-B1 models (dashed orange lines). MIPAS observations are also shown in the O₃ and H₂O plots (dashed green line).

confirms that in the global average modelled trends slightly underpredict the trends observed by the radiosondes (Austin et al., 2009). Overall, the response to volcanic events remains in general a challenge for most CCMs (SPARC, 2010).

3.2.8 Natural variability: Lower Stratosphere ozone

The 50 hPa ozone concentrations in NH spring and autumn are biased low.

Figure 11 shows climatological profiles and zonal-means of ozone from the model together with HALOE observations (same selection of months, latitudes and levels as in Fig. 7). CNRM-ACM was evidently an outlier at 50 hPa in tropical

to mid-latitudes, where mixing ratios were too low (negative bias up to 1 ppmv). There are several possible reasons for this. First, transport in CNRM-ACM that is too rapid, as shown by the REF-B1 age of air (see Fig. 4). However, plotting CNRM-ACM outputs from the CCMVal-2 REF-B2 simulation, that did not consider volcanic eruptions but had the same background aerosol loading as in 2000, does not confirm this hypothesis. Indeed, while the CNRM-ACM REF-B2 age of air (not shown) is very close to the CNRM-ACM REF-B1 age of air, the CNRM-ACM REF-B2 latitudinal distributions of ozone at 50 hPa in the tropics (as in Fig. 11d and e, not shown) are closer by around 0.5 ppmv to the HALOE observations. Thus the problem is not due to transport alone.

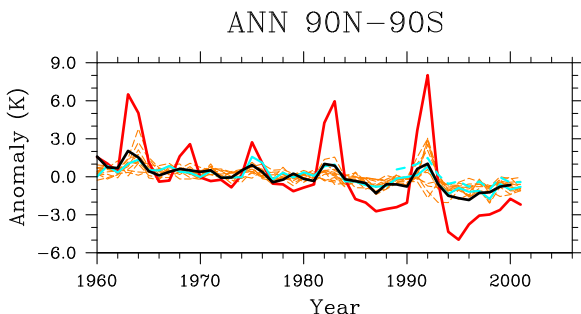


Fig. 10. Anomalies of annual mean global temperature at 50 hPa for ERA-40 (cyan solid line), ERA-Interim (dashed cyan line), CNRM-ACM (red line), CNRM-CCM (black line) and CCMVal-2 REF-B1 models (dashed orange lines). Anomalies are those w.r.t. the 1980–1989 period.

Another hypothesis could be that there are problems with the heterogeneous chemistry which lead to anomalous concentrations of ozone. However, the chemistry schemes in CNRM-ACM and CNRM-CCM are the same, and mixing ratios of O₃ from CNRM-CCM at 50 hPa are fully in line with the HALOE observations (see Fig. 11d and e). All this leads to the conclusion that, as underlined in Grant et al. (1994), tropical lower stratospheric ozone in the presence of volcanic eruptions is likely to be explained by a complex combination of dynamical and chemical processes.

3.2.9 Technical improvements

Finally, the last improvement we want to outline in this paper concerns the computing time, vital in climate modelling, required to perform the simulations. Running-time is significantly better for CNRM-CCM than for CNRM-ACM when we compare a T42/T42 CNRM-CCM simulation to a T42/T21 CNRM-ACM simulation, thus much coarser resolution for chemistry in the case of CNRM-ACM. The elapsed time on a Nec SX9 supercomputer that includes both CPU calculating time and time to transfer the outputs to the storage machine, which cannot be ignored when a large number of 3-D chemical fields needs to be archived (as often required in model inter-comparison projects), is of around 5.5 h for a T42/T42 CNRM-CCM yearly run, and around 55 h for a T42/T21 CNRM-ACM 1-yr long run. This difference can be explained in part by a better optimisation of the code for the transport of the chemical species, and is also linked to the additional computational burden of exchanging meteorological and ozone fields every 6 h between two different applications.

The CPU time of a run is multiplied by a factor of 2.5 running the CCM with the chemistry versus running it without, in the configuration we tested (T42 and 60 vertical levels). This factor enables additional simulations for “debugging” or sensitivity purposes to be performed.

3.3 Other validation results

The following results illustrate that the climatological state of the chemistry is satisfactory, both in the CNRM-ACM and in the CNRM-CCM simulations.

Figures 12 to 17 present, as in chapter 6 of SPARC (2010), mean annual cycles of selected species, including long-lived species (CH₄, H₂O, and CO), reservoirs (HCl, ClONO₂, HNO₃, and N₂O₅), two short-lived species (NO₂ and BrO), and O₃. Cycles are shown over several latitude bands (30° N–60° N, 60° S–30° S, and 15° S–15° N) at two levels, 50 hPa (see Figs. 12 to 14) and 1 hPa (see Figs. 15 to 17) to account for different controlling processes. Observations are those from HALOE for CH₄, H₂O, O₃ and HCl, from MIPAS for ClONO₂, HNO₃, N₂O₅ and NO₂, from SCIAMACHY for BrO, and from MLS for CO.

At 50 hPa the following appears: in mid-latitudes, both south and north, CNRM-CCM improves relative to CNRM-ACM for several species including CH₄, H₂O, O₃, HCl and HNO₃. This improvement, coherent with the improvements underlined in the various paragraphs of Sect. 3.2, is more or less marked depending on the chemical species. CNRM-CCM mixing ratios then fall within 1 standard deviation of the observed mean, which is not the case for a large number of CCMVal-2 models. A similar improvement is seen in the tropical latitudes except for HNO₃ where CNRM-CCM captures the HNO₃ annual cycle but its mixing ratios are biased low.

In contrast, CNRM-CCM NO₂ and N₂O₅ simulations at mid-latitudes are further from observations than CNRM-ACM simulations. They even span all the models presented at the high end. NO₂ and N₂O₅ mixing ratios appear less problematic in the tropics (see Fig. 14). As for CO, concentrations are lower for CNRM-CCM than for CNRM-ACM, but while they are close to the mean of the CCMVal-2 models they largely overestimate the MLS observations. We note that the ACE-FTS instrument climatology (instrument on-board SCISAT-1) has a flatter annual cycle than MLS (amplitude of 2 ppbv, see for instance SPARC, 2010 Fig. 6.16) and a larger annual mean mixing ratio (about 14.2 ppbv at mid-latitudes). These discrepancies between the two instruments are currently not fully understood as this is in the middle of the characteristic “C” shape of CO and is under the influence of both tropospheric and mesospheric transport. Finally, the CNRM-CCM simulation of ClONO₂ compares less well with observations than the CNRM-ACM simulation, though differences are small, and the CNRM-CCM simulation of BrO resembles that of CNRM-ACM with a negative bias over all the latitude bands shown. This negative bias is consistent with the CNRM simulations not including bromine from very short-lived species (that accounts for 5 pppt, see SPARC (2010) and references therein).

At 1 hPa, some statements made for the 50 hPa are still valid, i.e. improved CNRM-CCM CH₄ and H₂O, and deteriorated NO₂ and N₂O₅. This deterioration (mixing ratios

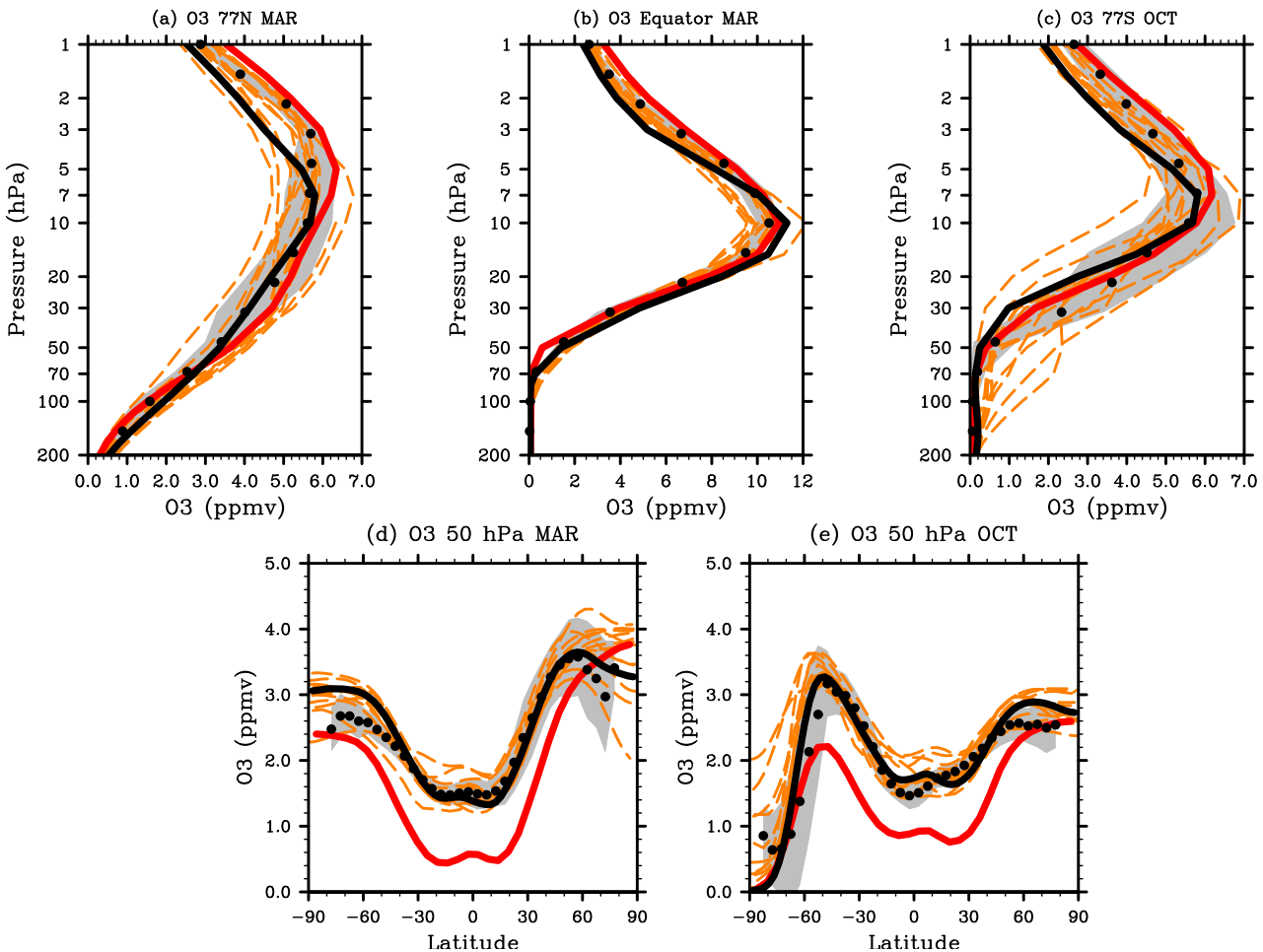


Fig. 11. Climatological (1992–2001) zonal-mean O₃ mixing (ppmv), for HALOE observations (black dots, with grey area showing $\pm 1\sigma$), CNRM-ACM (red line), CNRM-CCM (black line), and CCMVal-2 REF-B1 models (dashed orange lines). Vertical profiles at (a) 77° N in March, (b) 0° N in March, and (c) 77° S in October. Zonal-means at 50 hPa in (d) March and (e) October.

being too high) is more important in the winter months when CNRM-CCM is clearly an outlier and is coherent with the gradual conversion of NO₂ into N₂O₅ during the night. In addition, the climatologies of a number of species including CO, HCl, ClONO₂, BrO and HNO₃ from CNRM-CCM and CNRM-ACM are very close. Note that the satellite information is missing for HNO₃ (part of the year) and for BrO. The annual evolution of CO in the CNRM models does not seem to include the winter-time mid-latitude mesospheric input that some CCMVal-2 models represent to a certain extent. Observed (MIPAS) concentrations of ClONO₂ in the tropics are about 30 times lower than those in the models. However, the most disturbing diagnostic concerns the O₃ levels: while they are quite satisfactory in the mid-latitudes for CNRM-ACM, they are far too low for CNRM-CCM. CNRM-ACM and CNRM-CCM use the same chemical scheme, with identical photolysis rates (Sander et al., 2006; Madronich and Flocke, 1998; Brasseur et al., 1998);

however as CNRM-ACM did not participate in the photolysis benchmark of CCMVal-2 to evaluate CCM photolysis rates (see chapter 6 of SPARC, 2010), we have no detailed indication on the accuracy of our rates. A mis-representation of the temperatures at this altitude can explain at least in part the CNRM-CCM erroneous representation of ozone: indeed CNRM-CCM 1 hPa temperatures are biased high (5 to 9 K) compared to ERA-40 and ERA-Interim. Note that this temperature bias extends to the entire upper stratosphere in the 5–1 hPa range throughout the year (see Fig. S9 in the Supplement). At 1 hPa O₃ and temperatures appear very closely anti-correlated, indeed Khosravi et al. (1998) reported that constraining their model with analyzed temperatures (colder than those of their model) resulted in a significant increase of ozone near the stratopause. In our case, adding the chemistry on-line into the GCM resulted in better temperature fields near the stratopause (reducing the warm bias of the GCM), however other model processes need to be improved to end

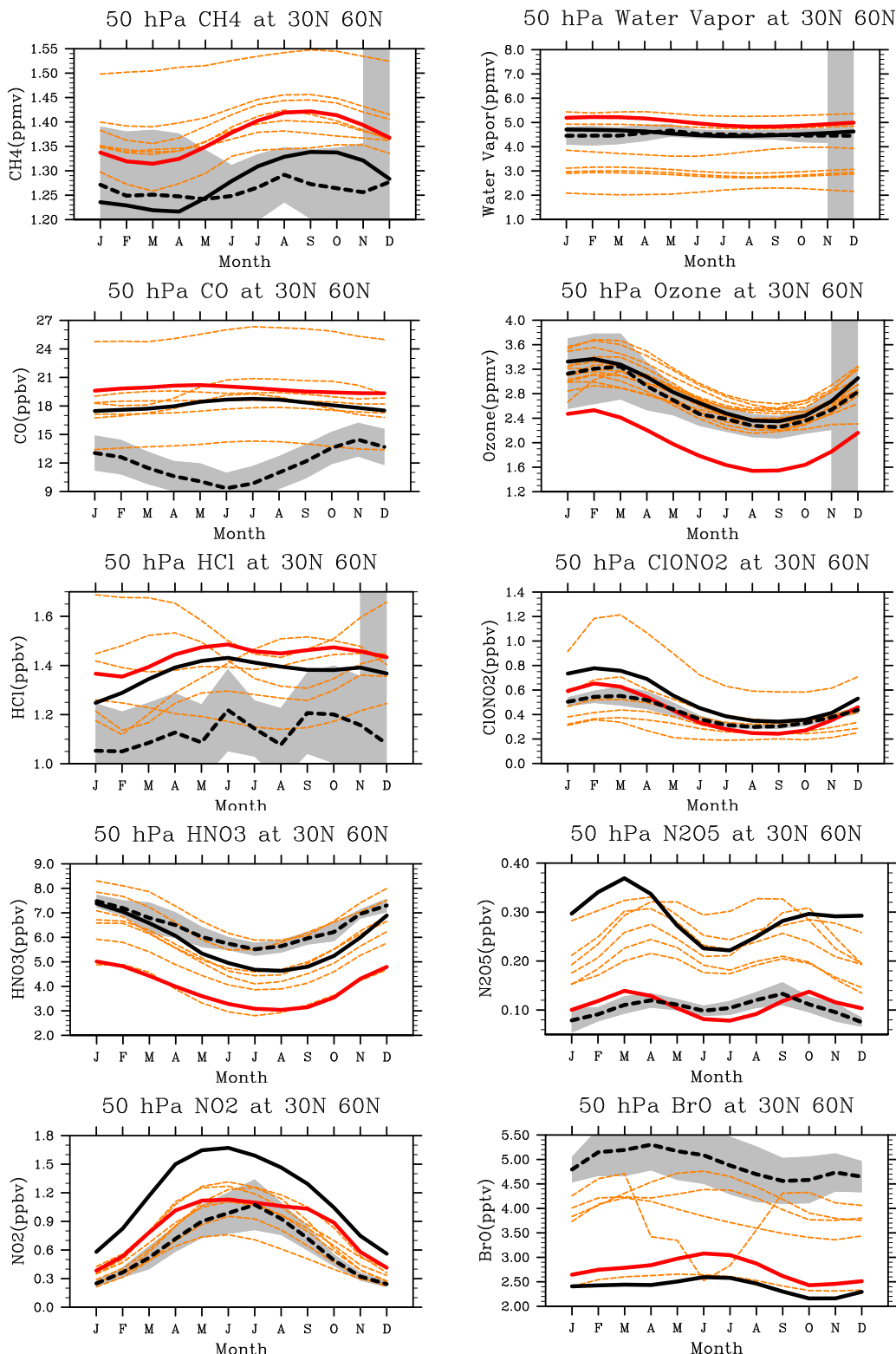


Fig. 12. Mean annual cycle at 50 hPa over 30° N–60° N for CH₄ (ppmv) and H₂O (ppmv) (first row), CO (ppbv) and O₃ (ppmv) (second row), HCl (ppbv) and ClONO₂ (ppbv) (third row), HNO₃ (ppbv) and N₂O₅ (ppbv) (fourth row), and NO₂ (ppbv) and BrO (pptv) (last row). Observations (dashed black line, $\pm 1\sigma$, see text), CNRM-ACM (red line), CNRM-CCM (black line) and CCMVal-2 REF-B1 models (dashed orange lines).

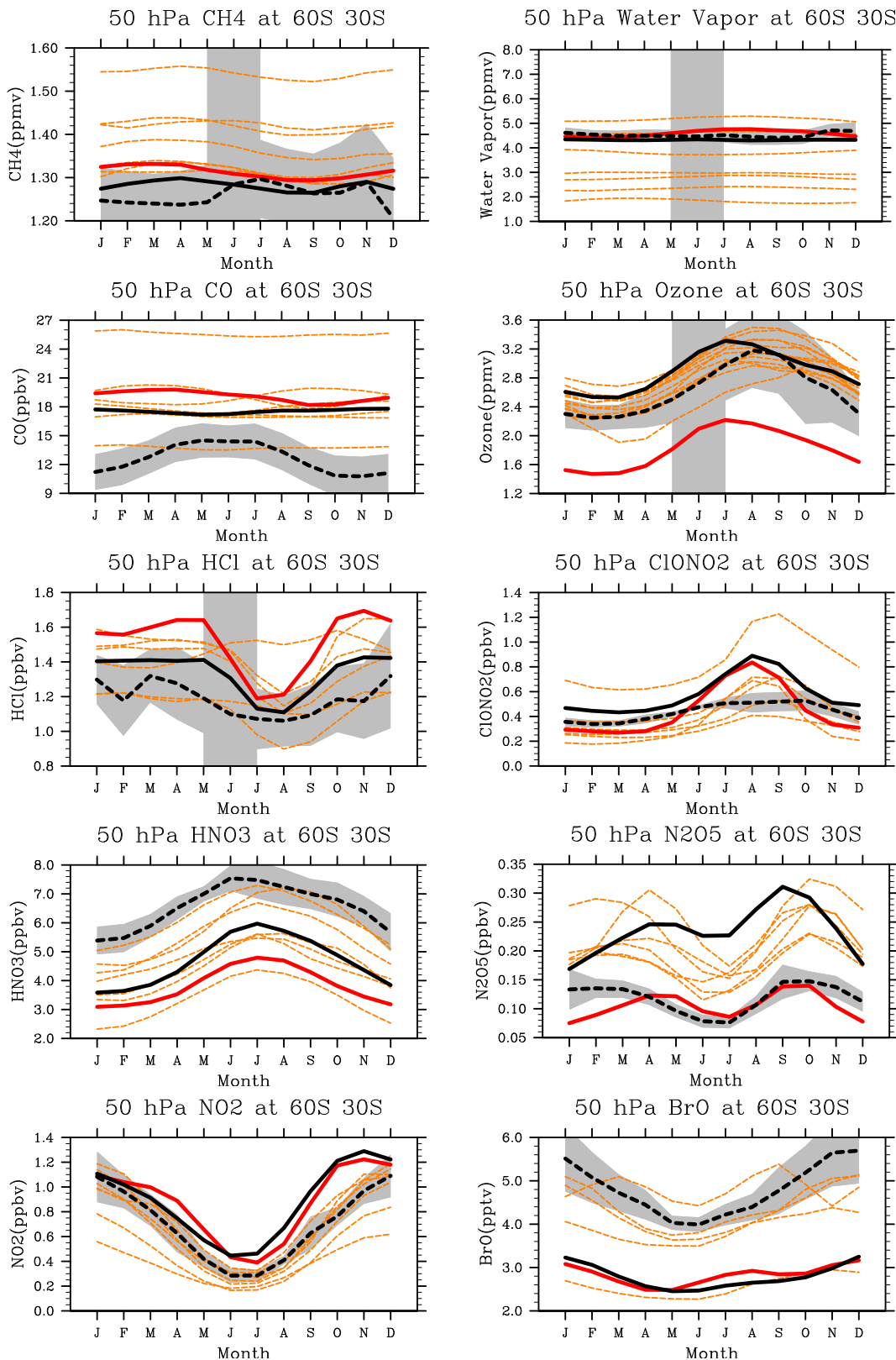
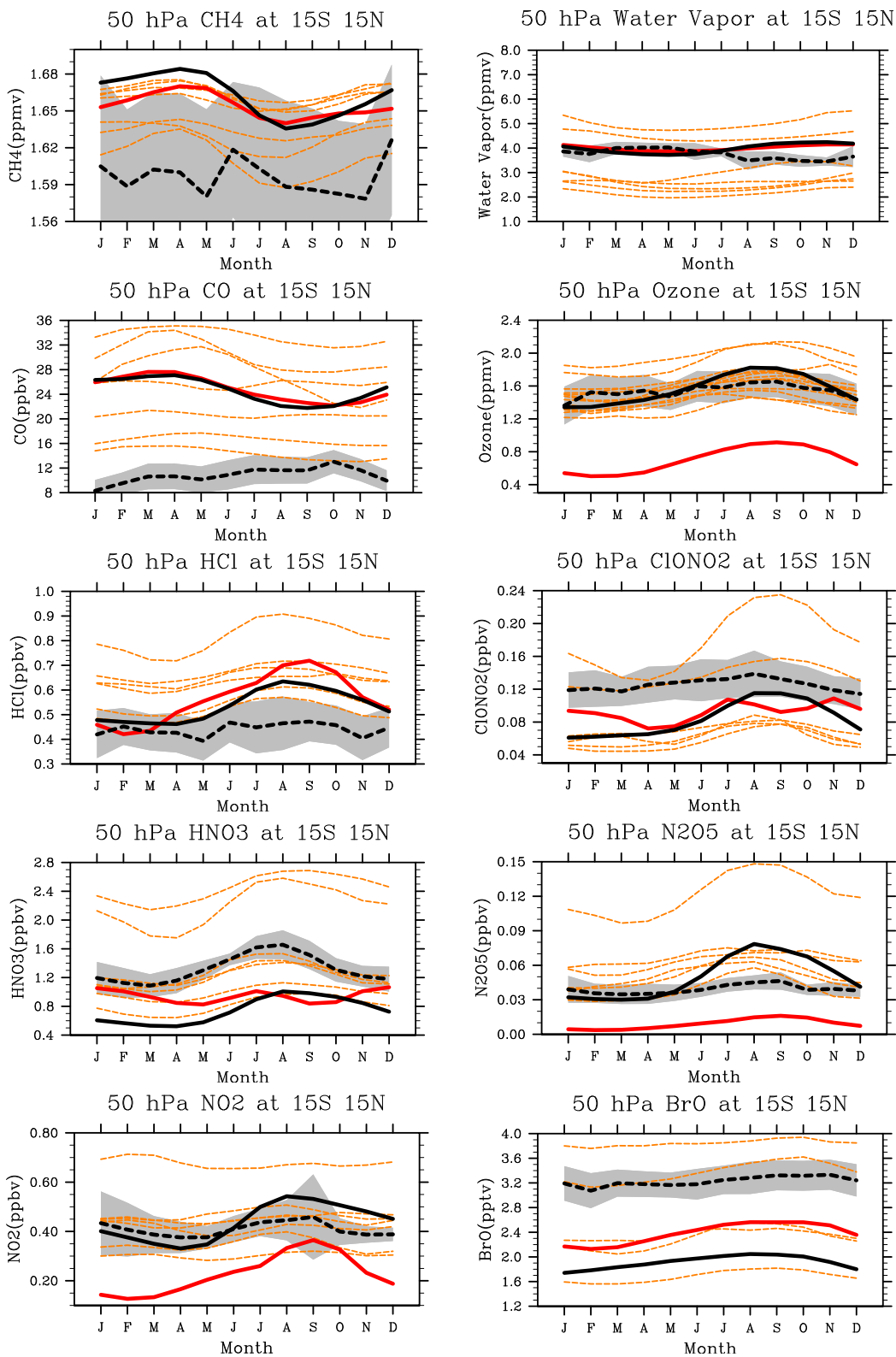


Fig. 13. Same as Fig. 12 at 50 hPa, 60° S–30° S.

**Fig. 14.** Same as Fig. 12 at 50 hPa, 15° S–15° N.

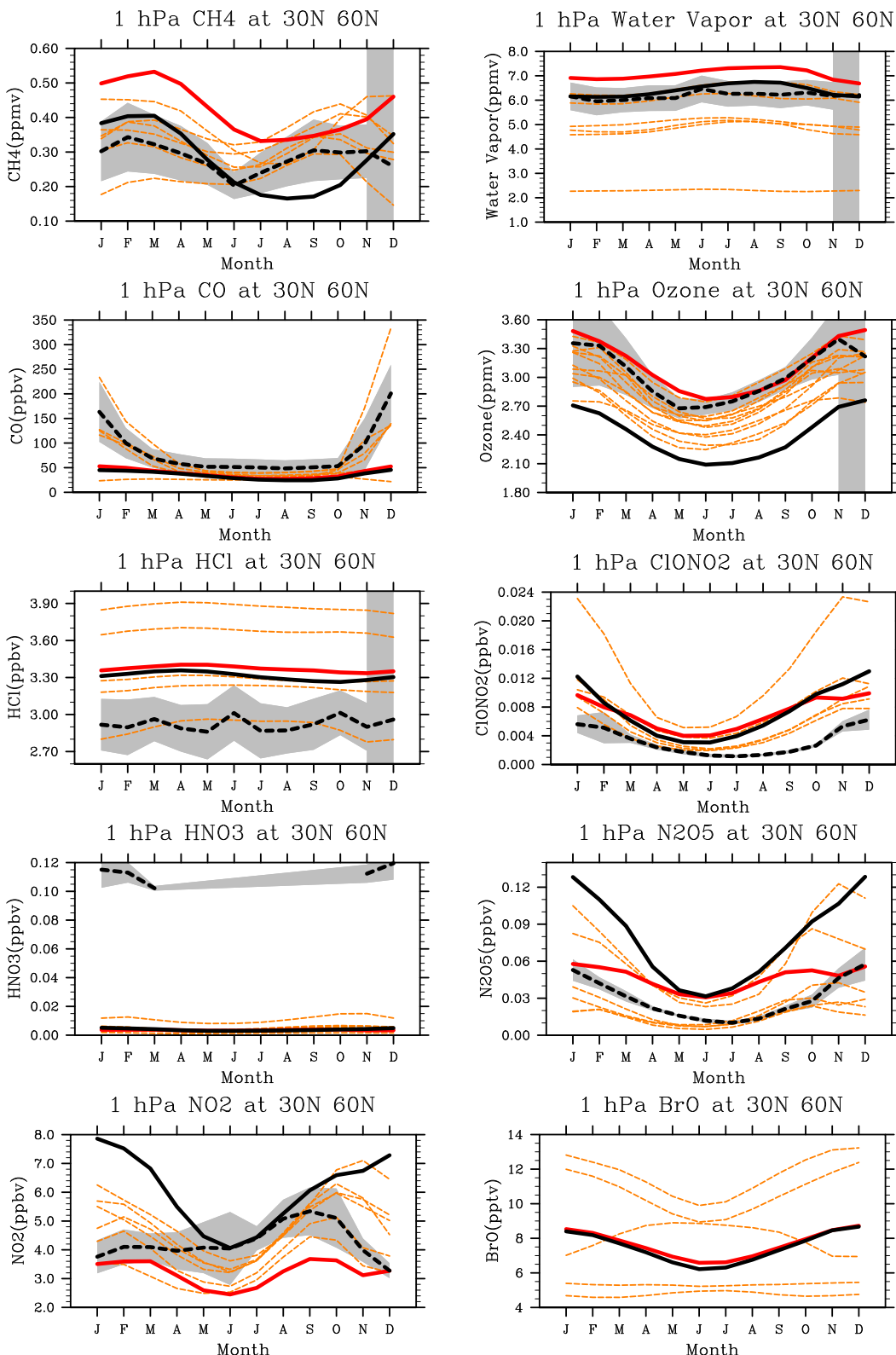
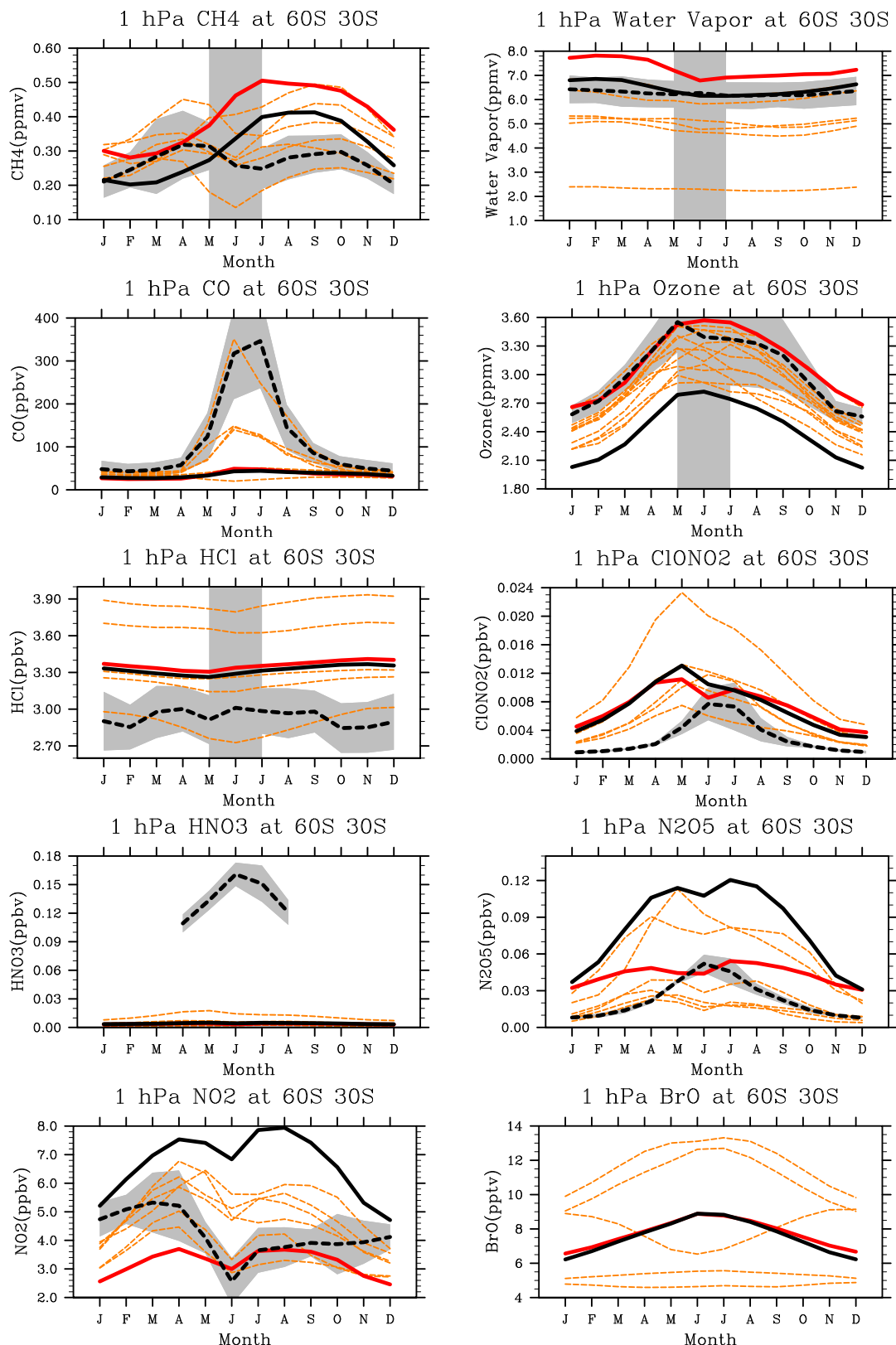


Fig. 15. Same as Fig. 12 at 1 hPa, 30° N–60° N.

**Fig. 16.** Same as Fig. 12 at 1 hPa, 60° S–30° S.

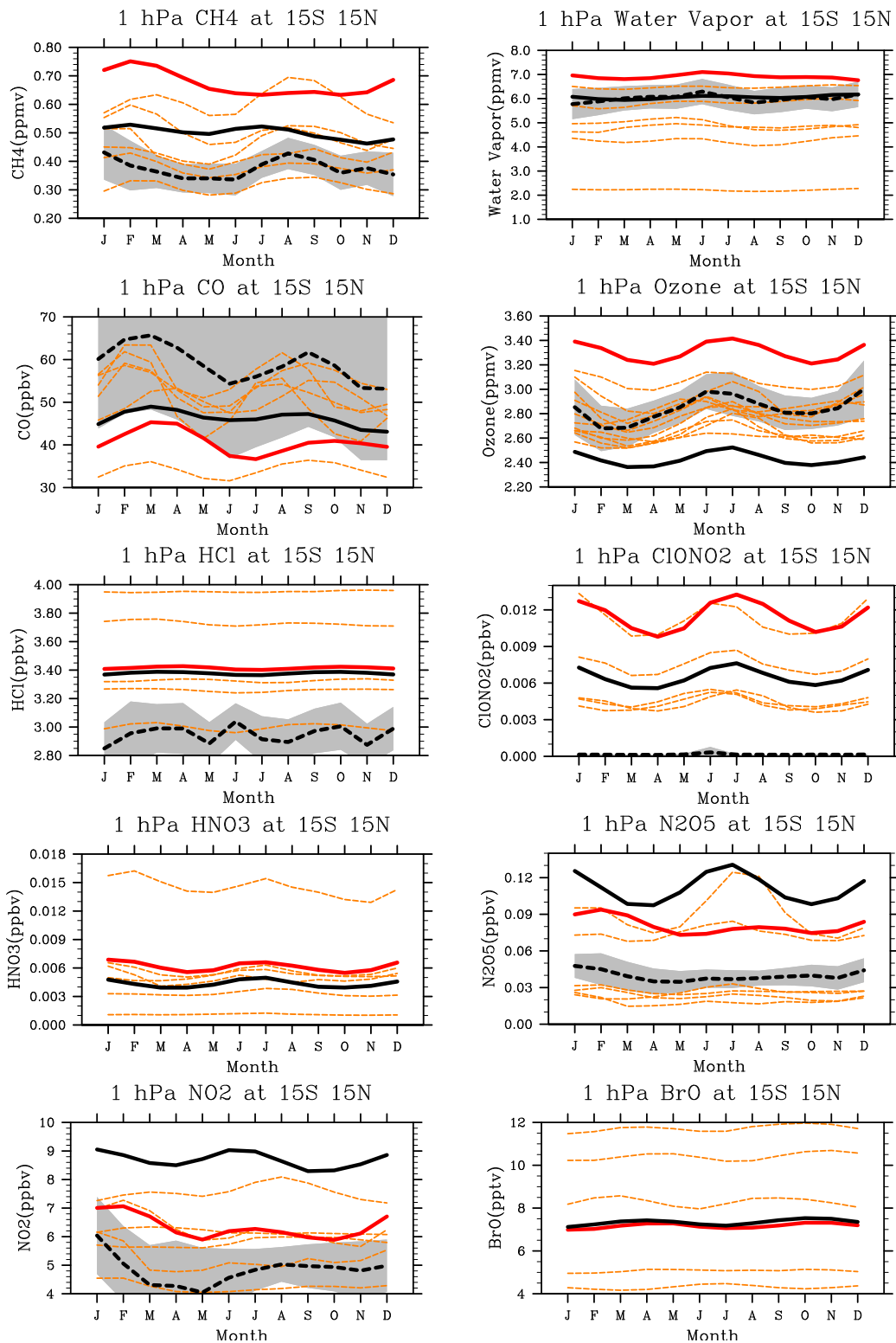


Fig. 17. Same as Fig. 12 at 1 hPa, 15° S–15° N.

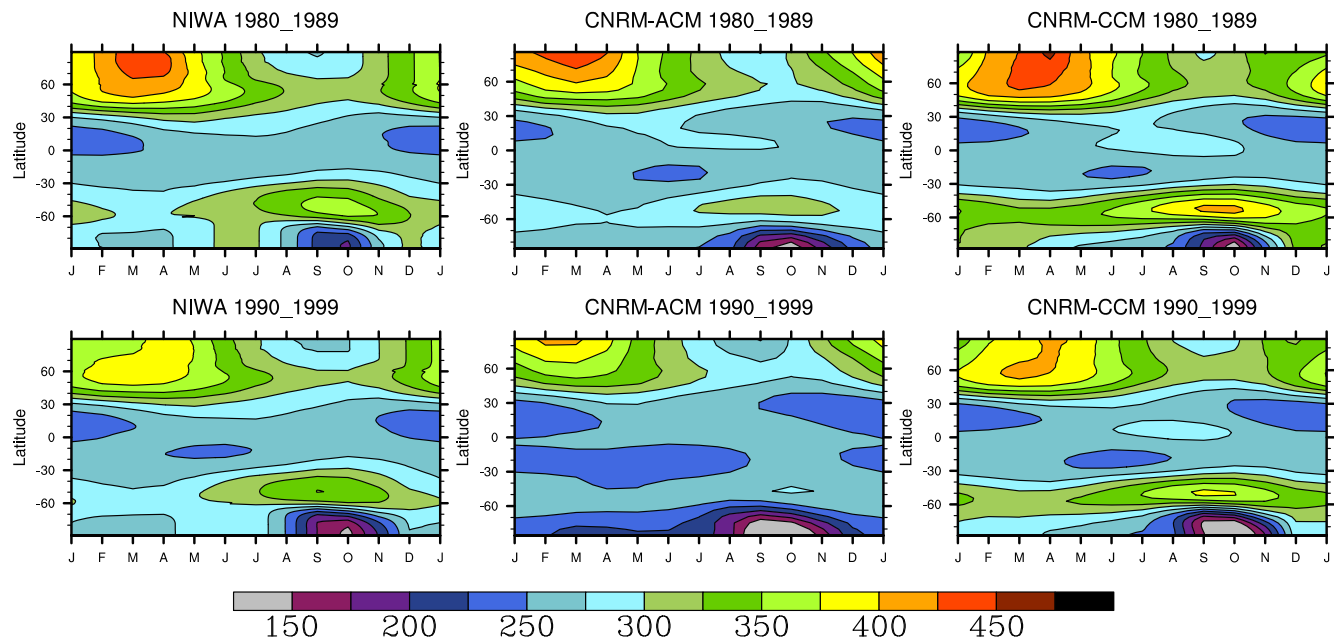


Fig. 18. Climatological monthly zonal total column ozone (DU) over two 10-yr periods, 1980–1989 (first row) and 1990–1999 (second row), for BSv2.7 observations (left column), CNRM-ACM (middle column) and CNRM-CCM (right column) simulations.

up with a correct temperature field that would be beneficial to the overall representation of the chemistry.

To conclude, we analyse results on the total column ozone. Figure 18 presents monthly zonal-means of NIWA observations and the CNRM-ACM and CNRM-CCM simulations valid for the 1980–1990 and 1990–2000 periods. The general patterns of the observations are better reproduced by CNRM-CCM than by CNRM-ACM, i.e., spring mid-latitude gradients, temporal evolution throughout the year of the tropical column, and confinement of the Antarctic vortex.

The negative trend in the column ozone at middle and high latitudes ($>45^\circ$) is evident in both observations and model outputs. The two CNRM models overestimate Antarctic ozone depletion, in all periods shown, in a lesser extent however for CNRM-CCM than for CNRM-ACM. This is linked to biases in temperature (see Fig. 1) that remain too low throughout the SH spring (see also Fig. 11e). Results are confirmed by looking at climatological yearly cycles of the total column ozone over high, mid and tropical latitude bands as in Tian et al. (2010) (see Fig. S12 in the Supplement). Overall, CNRM-CCM improves over CNRM-ACM and compares rather well with observations. CNRM-CCM shows a constant positive bias throughout the year at southern mid-latitudes (around 20 DU), at high latitudes it is within 1 standard deviation of the observations during part of the year. In both the 30° S– 30° N and the 30° – 60° N bands CNRM-CCM appears to be very realistic.

4 Synthesis of the CNRM-CCM model performance and outlook

In the previous section we showed that the new version of the CNRM Chemistry-Climate Model, so called CNRM-CCM, has a better performance than the previous version. We did not conduct a step-by-step analysis of what caused the differences between these two models, as that would be to a certain extent specific to our models, but changes in the radiation scheme led to a better mean meteorological stratosphere. Furthermore, introducing the chemistry on-line in the GCM reduced potential inconsistencies between the GCM and the chemical part of the model and resulted in a better representation of the various barriers to transport that are inherent to the stratospheric circulation. We analysed a 47-yr transient simulation (1960–2006) defined as the CCMVal-2 REF-B1 simulation (SPARC, 2010, Morgenstern et al., 2010a). Comparison of CNRM-CCM with meteorological reanalyses, satellite climatologies or CCMVal-2 models suggests that in many aspects CNRM-CCM performs well.

Stratospheric temperature biases in spring and winter at high latitudes are smaller or comparable to those of the CCMVal-2 models, with the exception of the upper stratosphere between 5 and 1 hPa where the model is too warm (5 to 9 K). This warm bias extends to all latitudes, is permanent throughout the year and simulations performed with no retroaction with the chemistry onto the radiative scheme reveal that it is intrinsic to the GCM itself. It is related undoubtedly to the radiative scheme (Morcrette et al., 2001)

that is in itself also perturbed by the 3-D distribution of the greenhouse gases. Bechtold et al. (2009) report on the reduction of this warm bias in the region of the stratopause due to a new climatology of greenhouse gases. In the end, a number of biases appear in the chemistry of the upper stratosphere. The model produces not enough O_3 , but too much NO_2 and N_2O_5 at 1 hPa and is then at the high end of the CCMVal-2 models.

Linked with this stratospheric distribution of temperatures, the other dynamical features analysed, transition to easterlies at $60^\circ S$, strength and position of the stratospheric jets, and pressure of the tropopause, compare favorably to the ERA-40 and ERA-Interim reanalyses. In contrast, the tropopause equatorial temperatures are biased low (maximum negative bias of 2.4 K) and are among the lowest within the CCMVal-2 models. This has been recognized as a common issue in CCMs (SPARC, 2010). However, the trend (1960–2000) of the global mean annual temperatures of the lower stratosphere (50 hPa), greatly affected by volcanic eruptions, is nicely captured by CNRM-CCM.

The characteristics of the transport appear to be quite accurately reproduced throughout the stratosphere, even though it is somewhat too rapid, and therefore the distributions of long-lived species, including CH_4 and HCl are well captured. Both the amplitude and the phase of the annual cycles of chemical species like O_3 and H_2O are well simulated in the UTLS where the effects of transport dominate when it is not the case indeed for all the CCMVal-2 models.

For the several other chemical species investigated, i.e. CO , $ClONO_2$, BrO and HNO_3 , the results do not reveal any major weakness in the model however the problems with reproducing the annual cycle for HNO_3 at 200 hPa $60^\circ S$ – $40^\circ S$ may require further investigation. Finally, our first analysis of the simulation of the total column ozone is quite encouraging.

As an overall picture of the agreement between the observations and the CNRM model outputs, in either phase and amplitude of the annual cycles, or of the vertical or latitudinal distributions, we plotted a Taylor diagram (Taylor, 2001) of the diagnostics analysed in the previous paragraphs of the paper (see Fig. S13 in the Supplement). For graphical purposes, negative correlation coefficients have been set to zero (see dots on the vertical axis), and normalized standard deviation higher than 1.7 have been set to 1.6. Furthermore, the identification of the individual diagnostics has been withdrawn from the figure as the objective was to get an overall picture of the performances of CNRM-CCM, and a possible comparison to CNRM-ACM. Though individual evolutions discussed in the paper between CNRM-ACM and CNRM-CCM are not identified in this Taylor diagram, interesting outcomes can be made: a number of diagnostics have poor skills, either because of a very low correlation with observations (see for instance CH_4 or CO in Fig. 13), and/or because of an amplitude of the signal far from that of the observations (standardized deviation lower than 0.5 or higher than 1.5, see

for instance H_2O in Fig. 9). In contrast, a substantial number of dots lie in the portion of the diagram close to the REF line (similar variances of models and observations), and delimited by a correlation coefficient higher than 0.9. Finally, it appears that CNRM-CCM has a larger number of satisfactory dots than CNRM-ACM. To assess whether both model versions were statistically different, we did not use the classical two-sample Student *t* Test as the results of both model versions are dependant (mostly due to the same forcings applied e.g., GHGs, SSTs), but we performed a one-sample Student *t* Test to test whether the differences of the two sample means were significantly different from zero (Wilks, 2006). We applied this test to each individual month of the annual profiles and each individual level of the vertical profiles of the diagnostics we present in this paper. The results we obtained appear in Tables S1 to S4 of the Supplement. Overall, these tables show that CNRM-ACM and CNRM-CCM are significantly different in most of the cases studied. For argument's sake, this is not the case, for example, for the equatorial temperature and water vapor at 100 hPa (see Table 2), but at the opposite all the results for O_3 in Table 3 reveal a significant difference.

We suggest that some of the chemical problems addressed above may be tackled by addressing issues related to the dynamics and the physics of the model. CNRM-CCM does not simulate at this stage intrinsically the QBO of the lower stratospheric equatorial winds (nor do most current CCMs, see SPARC, 2010). This has been identified as a major shortcoming by the CCMVal-2 project. Furthermore, the temperature of the higher stratosphere should be adjusted, possibly through the implementation of a more accurate radiation scheme in the short wavelengths. This is under consideration. Further developments of the model will also include the non-orographic aspects of the gravity waves, as well as the short-lived source gases containing bromine (WMO/UNEP, 2010). The latter will require to describe the tropospheric processes (e.g., emissions, convection, scavenging) that drive the evolution of these short-lived species. CNRM-CCM is planned for use in a variety of projects linked with the interactions between chemistry and climate, in particular in seasonal and decadal predictions, where it could possibly be coupled to an interactive ocean.

Supplementary material related to this

article is available online at:

<http://www.geosci-model-dev.net/4/873/2011/gmd-4-873-2011-supplement.pdf>.

Acknowledgements. We acknowledge the Chemistry-Climate Model Validation Activity (CCMVal) of the WCRP (World Climate Research Programme) SPARC (Stratospheric Processes and their Role in Climate) project for organising and coordinating the stratospheric model data analysis, and for providing the CCMVal Diagnostic Tool with which the figures of this article have been plotted. We particularly thank John Austin (AMTRAC3,

NOAA GFDL, USA), Chris Fisher and Doug Kinnison (CAM3.5, NCAR, USA), Hideharu Akiyoshi, Yousuke Yamashita and Tetsu Nakamura (CCSRNIES, NIES, Japan), David Plummer and John Scinocca (CMAM, EC, University of Toronto, York Univ., Canada), Martin Dameris and Hella Garny (E39CA, DLR, Germany), Steven Pawson and Richard Stolarski (GEOSCCM, NASA/GSFC, USA), Slimane Bekki and Marion Marchand (LMDZrepro, IPSL, France), Kiyotaka Shibata (MRI, MRI, Japan), Eugene Rozanov and Thomas Peter (SOCOL, PMOD/WRC and ETHZ, Switzerland), Eva Mancini and Giovanni Pitari (ULAQ, University of L'Aquila, Italy), John Austin and Greg Bodeker (UMETRAC, NIWA, NZ), Martyn Chipperfield, Sandip Dhomse and Wenshou Tian (UMSLIMCAT, University of Leeds, UK), Neal Butchart and Steven C. Hardiman (UMUKCA-METO, Met Office, UK), Peter Braesicke, Olaf Morgenstern, and John Pyle (UMUKCA-UCAM, University of Cambridge, UK), and Doug Kinnison, Andrew Gettelman, and Rolando Garcia (WACCM, NCAR, USA) for providing their results. We also acknowledge the British Atmospheric Data Centre (BADC) for collecting and archiving the CCMVal model output. ECMWF ERA-Interim data used in this study have been provided by ECMWF. The CCMVal-2 jet results presented in Fig. 3 were kindly provided by Michael Sigmond of the University of Toronto, the ENVISAT/MIPAS and SCIAMACHY satellite observations that appear in Figs. 12 to 17 by Sandip Dhomse of the University of Leeds. We also would like to thank Greg Bodeker of Bodeker Scientific for providing the combined total column ozone database. This work was partly supported by the French action "Les Enveloppes Fluides et l'Environnement" (LEFE) within the context of the MISSTERRE project. The authors would also like to acknowledge three anonymous referees for insightful comments that helped clarify and complete the manuscript.

Edited by: A. Lauer

References

- Ammann, C. M., Joos, F., Schimel, D. S., Otto-Bliesner, B. L., and Tomas, R. A.: Solar influence on climate during the past millennium: results from transient simulations with the NCAR Climate System Model, *Proc. Natl. Acad. Sci.*, 104, 3713–3718, 2007.
- Austin, J., Wilson, R. J., Akiyoshi, H., Bekki, S., Butchart, N., Claud, C., Fomichev, V. I., Forster, P., Garcia, R. R., Gillett, N. P., Keckhut, P., Langematz, U., Manzini, E., Nagashima, T., Randel, W. J., Rozanov, E., Shibata, K., Shine, K. P., Struthers, H., Thompson, D. W. J., Wu, F., and Yoden, S.: Coupled chemistry climate model simulations of stratospheric temperatures and their trends for the recent past, *Geophys. Res. Lett.*, 36, L13809, doi:10.1029/2009GL038462, 2009.
- Austin, J., Struthers, H., Scinocca, J., Plummer, D. A., Akiyoshi, H., Baumgaertner, A. J. G., Bekki, S., Bodeker, G. E., Braesicke, P., Brühl, C., Butchart, N., Chipperfield, M. P., Cugnet, D., Dameris, M., Dhomse, S., Frith, S., Garny, H., Gettelman, A., Hardiman, S. C., Jöckel, P., Kinnison, D., Kubin, A., Lamarque, J. F., Langematz, U., Mancini, E., Marchand, M., Michou, M., Morgenstern, O., Nakamura, T., Nielsen, J. E., Pitari, G., Pyle, J., Rozanov, E., Shepherd, T. G., Shibata, K., Smale, D., Teyssèdre, H., and Yamashita, Y.: Chemistry-climate model simulations of spring Antarctic ozone, *J. Geophys. Res.*, 115, D00M11, doi:10.1029/2009JD013577, 2010a.
- Austin, J., Scinocca, J., Plummer, D., Oman, L., Waugh, D., Akiyoshi, H., Bekki, S., Braesicke, P., Butchart, N., Chipperfield, M., Cugnet, D., Dameris, M., Dhomse, S., Eyring, V., Frith, S., Garcia, R. R., Garny, H., Gettelman, A., Hardiman, S. C., Kinnison, D., Lamarque, J. F., Mancini, E., Marchand, M., Michou, M., Morgenstern, O., Nakamura, T., Pawson, S., Pitari, G., Pyle, J., Rozanov, E., Shepherd, T. G., Shibata, K., Teyssèdre, H., Wilson, R. J., and Yamashita, Y.: Decline and recovery of total column ozone using a multimodel time series analysis, *J. Geophys. Res.*, 115, D00M10, doi:10.1029/2010JD013857, 2010b.
- Baldwin, M. P., Gray, L. J., Dunkerton, T. J., Hamilton, K., Haynes, P. H., Randel, W. J., Holton, J. R., Alexander, M. J., Hirota, I., Horinouchi, T., Jones, D. B. A., Kinnarsley, J. S., Marquardt, C., Sato, K., and Takahashi, M.: The Quasi-Biennial Oscillation, *Rev. Geophys.*, 39, 179–229, 2001.
- Bechtold, P., Orr, A., Morcrette, J.-J., Engelen, R., Flemming, J., and Janiskova, M.: Improvements in the stratosphere and mesosphere of the IFS, *ECMWF Newsletter No. 120*, Summer 2009.
- Bodeker, G. E., Shiona, H., and Eskes, H.: Indicators of Antarctic ozone depletion, *Atmos. Chem. Phys.*, 5, 2603–2615, doi:10.5194/acp-5-2603-2005, 2005.
- Bossuet, C., Déqué, M., and Cariolle, D.: Impact of a simple parameterization of convective gravity-wave drag in a stratosphere-troposphere general circulation model and its sensitivity to vertical resolution, *Ann. Geophys.*, 16, 238–249, doi:10.1007/s00585-998-0238-z, 1998.
- Bougeault, P.: A simple parametrisation of the large-scale effects of cumulus convection, *Mon. Weather Rev.*, 113, 2108–2121, 1985.
- Braesicke, P. and Pyle, J. A.: Sensitivity of dynamics and ozone to different representations of SSTs in the Unified Model, *Q. J. R. Meteorol. Soc.*, 130, 2033–2045, 2004.
- Brasseur, G. P., Hauglustaine, D. A., Walters, S., Rasch, P. J., Müller, J.-F., Granier, C., and Tie, X. X.: MOZART, a global chemical transport model for ozone and related chemical tracers, 1. Model description, *J. Geophys. Res.*, 103(D21), 28265–28289, 1998.
- Butchart, N., Charlton-Perez, A. J., Cionni, I., Hardiman, S. C., Haynes, P. H., Kruger, K., Kushner, P., Newman, P. A., Osprey, S. M., Perlitz, J., Sigmond, M., Wang, L., Akiyoshi, H., Austin, J., Bekki, S., Baumgaertner, A., Braesicke, P., Brühl, C., Chipperfield, M., Dameris, M., Dhomse, S., Eyring, V., Garcia, R., Garny, H., Gettelman, A., Jöckel, P., Kinnison, D., Lamarque, J.-F., Marchand, M., Michou, M., Morgenstern, O., Nakamura, T., Pawson, S., Peter, T., Plummer, D., Pyle, J., Rozanov, E., Scinocca, J., Shepherd, T. G., Shibata, K., Smale, D., Stolarski, R., Teyssèdre, H., Tian, W., Waugh, D., and Yamashita, Y.: Multi-model climate and variability of the stratosphere, *J. Geophys. Res.*, 116, D05102, doi:10.1029/2010JD014995, 2010.
- Cariolle, D. and Déqué, M.: Southern hemisphere medium-scale waves and total ozone disturbances in a spectral general circulation model, *J. Geophys. Res.*, 91, 10825–10846, 1986.
- Cariolle, D. and Morcrette, J.-J.: A linearized approach to the radiative budget of the stratosphere: influence of the ozone distribution, *Geophys. Res. Lett.*, 33, L05806, doi:10.1029/2005GL025597, 2006.
- Carslaw, K. S., Luo, B., Peter, T., and Clegg, S. L.: Vapour pressures of $H_2SO_4/HNO_3/HBr/H_2O$ solutions to low stratospheric temperatures, *Geophys. Res. Lett.*, 22, 247–250, 1995.
- Chapelon N., Douville, H., Kosuth, P., and Oki, T.: Off-line sim-

- ulation of the Amazon water balance: a sensitivity study with implications for GSWP, *Clim. Dynam.*, 19(2), 141–154, 2002.
- Dee D. and Uppala, S.: Variational bias correction in ERA-Interim, *ECMWF Newsletter*, No. 119, Spring 2009.
- Déqué, M.: Frequency of precipitation and temperature extremes over France in an anthropogenic scenario: model results and statistical correction according to observed values, *Glob. Planet. Change*, 57, 16–26, doi:10.1016/j.gloplacha.2006.11.030, 2007.
- Déqué, M., Dreveton, C., Braun, A., and Cariolle, D.: The ARPEGE-IFS atmosphere model: a contribution to the French community climate modelling, *Clim. Dynam.*, 10, 249–266, 1994.
- Douville, H., Royer, J.-F., and Mahfouf, J.-F.: A new snow parametrization for the Météo-France climate model, Part I: validation in stand-alone experiments, *J. Climate*, 12, 21–35, 1995.
- Douville H., Chauvin, F., Planton, S., Royer, J. F., Salas, D., and Tytca, M. S.: Sensitivity of the hydrological cycles to increasing amounts of greenhouse gases and aerosols, *Clim. Dynam.*, 20(1), 45–68, doi:10.1007/s00382-002-0259-3, 2002.
- Eyring, V., Kinnison, D. E., and Shepherd, T. G.: Overview of planned coupled chemistry-climate simulations to support upcoming ozone and climate assessments, *SPARC Newslett.*, 25, 11–17, 2005.
- Eyring, V., Butchart, N., Waugh, D. W., Akiyoshi, H., Austin, J., Bekki, S., Bodeker, G. E., Boville, B. A., Brühl, C., Chipperfield, M. P., Cordero, E., Dameris, M., Deushi, M., Fioletov, V. E., Frith, S. M., Garcia, R. R., Gettelman, A., Giorgi, M. A., Grewe, V., Jourdain, L., Kinnison, D. E., Mancini, E., Manzini, E., Marchand, M., Marsh, D. R., Nagashima, T., Newman, P. A., Nielsen, J. E., Pawson, S., Pitari, G., Plummer, D. A., Rozanov, E., Schraner, M., Shepherd, T. G., Shibata, K., Stolarski, R. S., Struthers, H., Tian, W., and Yoshiki, M.: Assessment of temperature, trace species, and ozone in chemistry-climate model simulations of the recent past, *J. Geophys. Res.*, 111, D22308, doi:10.1029/2006jd007327, 2006.
- Eyring, V., Waugh, D. W., Bodeker, G. E., Cordero, E., Akiyoshi, H., Austin, J., Beagley, S. R., Boville, B., Braesicke, P., Brühl, C., Butchart, N., Chipperfield, M. P., Dameris, M., Deckert, R., Deushi, M., Frith, S. M., Garcia, R. R., Gettelman, A., Giorgi, M., Kinnison, D. E., Mancini, E., Manzini, E., Marsh, D. R., Matthes, S., Nagashima, T., Newman, P. A., Nielsen, J. E., Pawson, S., Pitari, G., Plummer, D. A., Rozanov, E., Schraner, M., Scinocca, J. F., Semeniuk, K., Shepherd, T. G., Shibata, K., Steil, B., Stolarski, R., Tian, W., and Yoshiki, M.: Multimodel projections of stratospheric ozone in the 21st century, *J. Geophys. Res.*, 112, D16303, doi:10.1029/2006JD008332, 2007.
- Eyring, V., Chipperfield, M. P., Giorgi, M. A., Kinnison, D. E., Manzini, E., Matthes, K., Newman, P. A., Pawson, S., Shepherd, T. G., and Waugh, D. W.: Overview of the new CCMVal reference and sensitivity simulations in support of upcoming ozone and climate assessments and the planned SPARC CCMVal report, *SPARC Newsletter*, 30, 20–26, 2008.
- Gates, W. L., Boyle, J. S., Covey, C., Dease, C. G., Doutriaux, C. M., Drach, R. S., Fiorino, M., Gleckler, P. J., Hnilo, J. J., Marlais, S. M., Phillips, T. J., Potter, G. L., Santer, B. D., Sperber, K. R., Taylor, K. E., and Williams, D. N.: An overview of the results of the Atmospheric Model Intercomparison Project (AMIP I), *Bull. Am. Meteorol. Soc.*, 80, 29–55, 1999.
- Gettelman, A., Hegglin, M. I., Son, S.-W., Kim, J., Fujiwara, M., Birner, T., Kremser, S., Rex, M., Añel, J. A., Akiyoshi, H., Austin, J., Bekki, S., Braesike, P., Brühl, C., Butchart, N., Chipperfield, M., Dameris, M., Dhomse, S., Garny, H., Hardiman, S. C., Jöckel, P., Kinnison, D. E., Lamarque, J. F., Mancini, E., Marchand, M., Michou, M., Morgenstern, O., Pawson, S., Pitari, G., Plummer, D., Pyle, J. A., Rozanov, E., Scinocca, J., Shepherd, T. G., Shibata, K., Smale, D., Teyssèdre, H., and Tian, W.: Multi-model Assessment of the Upper Troposphere and Lower Stratosphere: Tropics and Trends, *J. Geophys. Res.*, 115, D00M08, doi:10.1029/2009JD013638, 2010.
- Grant, W., Browell, E. V., Fishman, J., Brackett, V. G., Veiga, R. E., Nganga, D., Minga, A., Cros, B., Butler, C. F., Fenn, M. A., Long, C. S., and Stowe, L. L.: Aerosol associated changes in tropical stratospheric ozone following the eruption of Mount Pinatubo, *J. Geophys. Res.*, 99(D4), 8197–8211, 1994.
- Groß, J.-U. and Russell III, James M.: Technical note: A stratospheric climatology for O₃, H₂O, CH₄, NO_x, HCl and HF derived from HALOE measurements, *Atmos. Chem. Phys.*, 5, 2797–2807, doi:10.5194/acp-5-2797-2005, 2005.
- Hegglin, M. I., Gettelman, A., Hoor, P., Krichevsky, R., Manney, G. L., Pan, L. L., Son, S.-W., Stiller, G., Tilmes, S., Walker, K. A., Eyring, V., Shepherd, T. G., Waugh, D., Akiyoshi, H., Añel, J. A., Austin, J., Baumgaertner, A., Bekki, S., Braesicke, P., Brühl, C., Butchart, N., Chipperfield, M., Dameris, M., Dhomse, S., Frith, S., Garny, H., Hardiman, S. C., Jöckel, P., Kinnison, D. E., Lamarque, J. F., Mancini, E., Michou, M., Morgenstern, O., Nakamura, T., Olivie, D., Pawson, S., Pitari, G., Plummer, D. A., Pyle, J. A., Rozanov, E., Scinocca, J. F., Shibata, K., Smale, D., Teyssèdre, H., Tian, W., and Yamashita, Y.: Multi-Model Assessment of the Upper Troposphere and Lower Stratosphere: Extra-tropics, *J. Geophys. Res.*, 115, D00M09, doi:10.1029/2010JD013884, 2010.
- Johns, T. C., Royer, J.-F., Hoschel, I., Huebener, H., Roeckner, E., Manzini, E., May, W., Dufresne, J.-L., Ottera, O. H., van Vuuren, D. P., Salas, D., Melia, Y., Giorgi, M., Deniel, S., Yang, S., Fogli, P. G., Korper, J., Tjiputra, J. F., Hewitt, C. D.: Climate change under aggressive mitigation: The ENSEMBLES multi-model experiment, *Clim. Dynam.*, 1–29, doi:10.1007/s00382-011-1005-5, 2011.
- Josse, B., Simon, P., and Peuch, V.-H.: Rn–222 global simulations with the multiscale CTM MOCAGE, *Tellus*, 56B, 339–356, 2004.
- Jourdain, L., Bekki, S., Lott, F., and Lefèvre, F.: The coupled chemistry-climate model LMDz-REPROBUS: description and evaluation of a transient simulation of the period 1980–1999, *Ann. Geophys.*, 26, 1391–1413, doi:10.5194/angeo-26-1391-2008, 2008.
- Khosravi, R., Brasseur, G. P., Smith, A. K., Rusch, D. W., Waters, J. W., and Russell III, J. M.: Significant reduction in the stratospheric ozone deficit using a three-dimensional model constrained with UARS data, *J. Geophys. Res.*, 103, 16203–16219, 1998.
- Lee, J. N., Wu, D. L., Manney, G. L., Schwartz, M. J., Lambert, A., Livesey, N. J., Minschwaner, K. R., Pumphrey, H. C., and Read, W. G.: Aura Microwave Limb Sounder Observations of the Polar Middle Atmosphere: Dynamics and Transport of CO and H₂O, *J. Geophys. Res.*, 116, D05110, doi:10.1029/2010JD014608, 2011.
- Lefèvre, F., Brasseur, G. P., Folkens, I., Smith, A. K., and Simon, P.: Chemistry of the 1991–1992 stratospheric winter: threedimensional modeling of the seasonal cycle, *J. Geophys. Res.*, 116, D05111, doi:10.1029/2010JD014609, 2011.

- dimensional model simulations, *J. Geophys. Res.*, 99, 8183–8195, 1994.
- Liu, C., Zipser, E., Garrett, T., Jiang, J. H., and Su, H.: How do the water vapor and carbon monoxide tape recorders start near the tropical tropopause?, *Geophys. Res. Lett.*, 34, L09804, doi:10.1029/2006GL029234, 2007.
- Lott, F.: Alleviation of stationary biases in a GCM through a mountain drag parametrization scheme and a simple representation of mountain lift forces, *Mon. Weather Rev.* 125, 788–801, 1999.
- Lott, F. and Miller, M. J.: A new subgrid-scale orographic drag parametrization: its formulation and testing, *Quart. J. Roy. Meteor. Soc.*, 123, 101–127, 1997.
- Louis, J., Tiedtke, M., and Geleyn, J.: A short history of the operational PBL-parameterization at ECMWF, ECMWF Workshop on Planetary Boundary Layer Parameterization, ECMWF, Reading, 59–80, 1982.
- Madronich, S. and Flocke, S.: The role of solar radiation in atmospheric chemistry, in: *Handbook of Environmental Chemistry*, edited by: Boule, P., 1–26, Springer-Verlag, New York, 1998.
- Mahfouf, J.-F., Manzi, O., Noilhan, J., Giordani, H., and Déqué, M.: The land surface scheme ISBA within the Météo-France climate model ARPEGE, Part I: Implementation and preliminary results, *J. Climate*, 8, 2039–2057, 1995.
- Mascart, P., Noilhan, J., and Giordani, H.: A modified parameterization of flux-profile relationships in the surface layer using different roughness length values for heat and momentum, *Bound.-Lay. Meteorol.*, 72, 331–344, 1995.
- Maynard K. and Royer, J. F.: Sensitivity of a general circulation model to land surface parameters in African tropical deforestation experiment, *Clim. Dynam.*, 22, 555–572, 2004.
- Morcrette, J.-J.: Radiation and cloud radiative properties in the ECMWF operational 1388 weather forecast model, *J. Geophys. Res.*, 96, 9121–9132, 1991.
- Morcrette J.-J., Mlawer, E. J., Iacono, M. J., and Clough, S. A.: Impact of the radiation-transfer scheme RRTM in the ECMWF forecasting system, ECMWF Newsletter No. 91, Summer 2001.
- Morgenstern O., Giorgetta, M. A., Shibata, K., Eyring, V., Waugh, D. W., G. Shepherd, T., Akiyoshi, H., Austin, J., Baumgaertner, A. J. G., Bekki, S., Braesicke, P., Brühl, C., Chipperfield, M. P., Cugnet, D., Dameris, M., Dhomse, S., Frith, S. M., Garny, H., Gettelman, A., Hardiman, S. C., Hegglin, M. I., Jöckel, P., Kinnison, D. E., Lamarque, J.-F., Mancini, E., Manzini, E., Marchand, M., Michou, M., Nakamura, T., Nielsen, J. E., Olivie, D., Pitari, G., Plummer, D. A., Rozanov, E., Scinocca, J. F., Smale, D., Strahan, S., Teyssèdre, H., Toohey, M., Tian, W., and Yamashita, Y.: Review of present-generation stratospheric chemistry-climate models and associated external forcings, *J. Geophys. Res.*, 115, D00M02, doi:10.1029/2009JD013728, 2010a.
- Morgenstern, O., Akiyoshi, H., Bekki, S., Braesicke, P., Butchart, N., Chipperfield, M. P., Cugnet, D., Deushi, M., Dhomse, S. S., Garcia, R. R., Gettelman, A., Gillett, N. P., Hardiman, S. C., Jumelet, J., Kinnison, D. E., Lamarque, J.-F., Lott, F., Marchand, M., Michou, M., Nakamura, T., Olivie, D., Peter, T., Plummer, D., Pyle, J. A., Rozanov, E., Saint-Martin, D., Scinocca, J. F., Shibata, K., Sigmond, M., Smale, D., Teyssèdre, H., Tian, W., Volodire, A., and Yamashita, Y.: Anthropogenic forcing of the Northern Annular Mode in CCMVal-2 models, *J. Geophys. Res.*, 115, D00M03, doi:10.1029/2009JD013347, 2010b.
- Noilhan, J. and Planton, S.: A simple parameterization of land surface processes for meteorological models, *Mon. Weather Rev.*, 117, 536–549, 1989.
- Oman, L. D., Plummer, D. A., Waugh, D. W., Austin, J., Scinocca, J. F., Douglass, A. R., Salawitch, R. J., Carty, T., Akiyoshi, H., Bekki, S., Braesicke, P., Butchart, N., Chipperfield, M. P., Cugnet, D., Dhomse, S., Eyring, V., Frith, S., Hardiman, S. C., Kinnison, D. E., Lamarque, J.-F., Mancini, E., Marchand, M., Michou, M., Morgenstern, O., Nakamura, T., Nielsen, J. E., Olivie, D., Pitari, G., Pyle, J., Rozanov, E., Shepherd, T. G., Shibata, K., Stolarski, R. S., Teyssèdre, H., Tian, W., Yamashita, Y., and Ziemke, J. R.: Multimodel assessment of the factors driving stratospheric ozone evolution over the 21st century, *J. Geophys. Res.*, 115, D24306, doi:10.1029/2010JD014362, 2010.
- Randel, W., Chanin, M.-L., and Michaut, C.: SPARC Intercomparison of Middle Atmosphere Climatologies, SPARC Report No. 3, 96 pp., 2002.
- Randel, W., Udelhofen, P., Fleming, E., Geller, M., Gelman, M., Hamilton, K., Karoly, D., Ortland, D., Pawson, S., Swinbank, R., Wu, F., Baldwin, M., Chanin, M.-L., Keckhut, P., Labitzke, K., Remsberg, E., Simmons, A., and Wu, D.: The SPARC Intercomparison of Middle Atmosphere Climatologies, *J. Climate*, 17, 986–1003, 2004.
- Rayner, N. A., Parker, D. E., Horton, E. B., Folland, C. K., Alexander, L. V., Rowell, D. P., Kent, E. C., and Kaplan, A.: Global analyses of sea surface temperature, sea ice, and night marine air temperature since the late nineteenth century, *J. Geophys. Res.*, 108, 4407, doi:10.1029/2002JD002670, 2003.
- Ricard, J.-L. and Royer, J.-F.: A statistical cloud scheme for use in a AGCM, *Ann. Geophys.*, 11, 1095–1115, 1993.
- Saint-Martin, D.: Etude comparative du rôle de la dynamique et de la chimie dans la modélisation de l'atmosphère moyenne, Ph.D thesis, Université Toulouse III Paul Sabatier, 2010.
- Sander, S. P., Friedl, R. R., Golden, D. M., Kurylo, M. J., Moortgat, G. K., Keller-Rudek, H., Wine, P. H., Ravishankara, A. R., Kolb, C. E., Molina, M. J., Finlayson-Pitts, B. J., Huie, R. E., and Orkin, V. L.: Chemical kinetics and photochemical data for use in atmospheric studies, Evaluation Number 15, JPL Publication 06-2, Jet Propulsion Laboratory, Pasadena, 2006.
- Schranner, M., Rozanov, E., Schnadt Poberaj, C., Kenzelmann, P., Fischer, A. M., Zubov, V., Luo, B. P., Hoyle, C. R., Egorova, T., Fueglister, S., Brönnimann, S., Schmutz, W., and Peter, T.: Technical Note: Chemistry-climate model SOCOL: version 2.0 with improved transport and chemistry/microphysics schemes, *Atmos. Chem. Phys.*, 8, 5957–5974, doi:10.5194/acp-8-5957-2008, 2008.
- Simmons A., Uppala, S., Dee, D., and Kobayashi, S.: ERA-Interim: New ECMWF reanalysis products from 1989 onwards, ECMWF Newsletter, No. 110, Winter 2006.
- Solomon, S., Qin, D., Manning, M., Chen, Z., Marquis, M., Averyt, K. B., Tignor, M., and Miller, H. L.: IPCC, 2007: *Climate Change 2007: The Physical Science Basis. Contribution of Working Group I to the Fourth Assessment Report of the Intergovernmental Panel on Climate Change*, Cambridge University Press, Cambridge, United Kingdom and New York, NY, USA, 996 pp., 2007.
- Son, S.-W., Gerber, E. P., Perlitz, J., Polvani, L. M., Gillett, N. P., Seo, K.-H., Eyring, V., Shepherd, T. G., Waugh, D., Akiyoshi, H., Austin, J., Baumgaertner, A., Bekki, S., Braesicke, P., Brühl, C., Butchart, N., Chipperfield, M. P., Cugnet D., Dameris, M.,

- Dhomse, S., Frith, S., Garny, H., Garcia, R., Hardiman, S. C., Jöckel, P., Lamarque, J.-F., Mancini, E., Marchand, M., Michou, M., Nakamura, T., Morgenstern, O., Pitari, G., Plummer, D. A., Pyle, J., Rozanov, E., Scinocca, J. F., Shibata, K., Smale, D., Teyssèdre, H., Tian, W., and Yamashita, Y.: Impact of Stratospheric Ozone on Southern Hemisphere Circulation Change: A Multimodel Assessment, *J. Geophys. Res.*, 15, D00M07, doi:10.1029/2010JD014271, 2010.
- SPARC CCMVal, SPARC CCMVal Report on the Evaluation of Chemistry-Climate Models: edited by: Eyring, V., Shepherd, T. G., and Waugh, D. W., SPARC Report No. 5, WCRP-132, WMO/TD-No. 1526, available at: <http://www.atmosp.physics.utoronto.ca/SPARC>, 2010.
- Swingedouw, D., Terray, L., Cassou, C., Volodire, A., Salas, D., Melia, Y., and Servonnat, J.: Natural forcing of climate during the last millennium: Fingerprint of solar variability, *Clim. Dynam.*, 36, 1349–1364, doi:10.1007/s00382-010-0803-5, 2010.
- Taylor, K. E.: Summarizing multiple aspects of model performance in a single diagram, *J. Geophys. Res.*, 106(D7), 7183–7192, 2001.
- Tegen, I., Hoorig, P., Chin, M., Fung, I., Jacob, D., and Penner, J.: Contribution of different aerosol species to the global aerosol extinction optical thickness: Estimates from model results, *J. Geophys. Res.*, 102, 23895–23915, 1997.
- Teyssèdre, H., Michou, M., Clark, H. L., Josse, B., Karcher, F., Olivié, D., Peuch, V.-H., Saint-Martin, D., Cariolle, D., Attié, J.-L., Nédélec, P., Ricaud, P., Thouret, V., van der A, R. J., Volz-Thomas, A., and Chéroux, F.: A new tropospheric and stratospheric Chemistry and Transport Model MOCAGE-Climat for multi-year studies: evaluation of the present-day climatology and sensitivity to surface processes, *Atmos. Chem. Phys.*, 7, 5815–5860, doi:10.5194/acp-7-5815-2007, 2007.
- Tian, W., Chipperfield, M. P., Stevenson, D. S., Damoah, R., Dhomse, S., Dudhia, A., Pumphrey, H., and Bernath, P.: Effects of stratosphere-troposphere chemistry coupling on tropospheric ozone, *J. Geophys. Res.*, 115, D00M04, doi:10.1029/2009JD013515, 2010.
- Uppala S. M., Källberg, P. W., Simmons, A. J., Andrae, U., Da Costa Bechtold, V., Fiorino, M., Gibson, J. K., Haseler, J., Hernandez, A., Kelly, G. A., Li, X., Onogi, K., Saarinen, S., Sokka, N., Allan, R. P., Andersson, E., Arpe, K., Balmaseda, M. A., Beljaars, A. C. M., Van De Berg, L., Bidlot, J., Bormann, N., Caires, S., Chevallier, F., Dethof, A., Dragosavac, M., Fisher, M., Fuentes, M., Hagemann, S., Holm, E., Hoskins, B. J., Isaksen, L., Janssen, P. A. E. M., Jenne, R., McNally, A. P., Mahfouf, J.-F., Morcrette, J.-J., Rayner, N. A., Saunders, R. W., Simon, P., Sterl, A., Trenberth, K. E., Untch, A., Vasiljevic, D., Viterbo, P., and Woollen, J.: The ERA-40 reanalysis, *Q. J. R. Meteorol. Soc.*, 131, 2961–3012, 2005.
- Uppala S., Dee, D., Kobayashi, S., Berrisford, P., and Simmons, A.: Towards a climate data assimilation system: status update of ERA-Interim, *ECMWF Newsletter* No. 115, Spring 2008.
- Volodire, A. and Royer, J. F.: Climate sensitivity to tropical land surface changes with coupled versus prescribed SSTs, *Clim. Dynam.*, 24, 843–862, 2005.
- Volodire A., Sanchez-Gomez, E., Salas y Méria, D., Decharme, B., Cassou, C., Sé nési, S., Valcke, S., Beau, I., Alias, A., Chevalier, M., Déqué, M., Deshayes, J., Douville, H., Fernandez, E., Madec, G., Maisonneuve, E., Moine, M.-P., Planton, S., Saint-Martin, D., Szopa, S., Tytca, S., Alkama, R., Belamari, S., Braun, A., Coquart, L., and Chauvin, F.: The CNRM-CM5.1 global climate model: description and basic evaluation, *Clim. Dynam.*, submitted, 2011.
- Wilks, D. S.: Statistical methods in the Atmospheric Sciences, 2nd Edn., Academic Press, 627 pp., 2006.
- Williams, J. E., Scheele, R., Van Velthoven, P., Bouarar, I., Law, K., Josse, B., Peuch, V.-H., Yang, X., Pyle, J., Thouret, V., Barret, B., Liouesse, C., Hourdin, F., Szopa, S., and Cozic, A.: Global Chemistry simulations in the AMMA-Model Intercomparison project, *Bull. Am. Meteor. Soc.*, 91, 611–624, 2010.
- Williamson, D. L. and Rash, P. J.: Two-dimensional semi-lagrangian transport with shape-preserving interpolation, *Mon. Weather Rev.*, 117, 102–129, 1989.
- WMO, World Meteorological Organization: Scientific assessment of stratospheric ozone, World Meteorological Organization, Global Ozone Research and Monitoring Project, Report 52, Geneva, Switzerland, 2010.